

**PERFORMANCE ANALYSIS OF BEAMFORMING FOR  
FEMTOCELLULAR APPLICATIONS**

by

Wooyoung Ryu

A thesis submitted to the Faculty of the University of Delaware in partial fulfillment of the requirements for the degree of Master of Science in Electrical and Computer Engineering

Summer 2010

© 2010 Wooyoung Ryu  
All Rights Reserved

**PERFORMANCE ANALYSIS OF BEAMFORMING FOR  
FEMTOCELLULAR APPLICATIONS**

by

Wooyoung Ryu

Approved: \_\_\_\_\_  
Leonard J. Cimini, Jr., Ph.D.  
Professor in charge of thesis on behalf of the Advisory Committee

Approved: \_\_\_\_\_  
Kenneth Barner, Ph.D.  
Chair of the Department of Electrical and Computer Engineering

Approved: \_\_\_\_\_  
Michael J. Chajes, Ph.D.  
Dean of the College of Engineering

Approved: \_\_\_\_\_  
Debra Hess Norris, M.S.  
Vice Provost for Graduate and Professional Education

## ACKNOWLEDGEMENTS

There are many people who gave me a lot of advices during my study. Above all, I would like to express my sincere gratitude to my advisor, Dr. Leonard J. Cimini, Jr. I could have not finished this thesis without his considerable guidance, and invaluable technical comments. It was one of the greatest opportunities in my life to study and research under his supervision. I will never forget this experience with him. Also, I am grateful to Chenzi Jiang, a graduate student at Delaware. She provided precious technical comments and fruitful discussion during this research.

I also would like to express my truthful royalty to Korean Navy. They gave me a great chance to study in University of Delaware with funding. Recently, during my research, the Korean Navy had suffered from the worst naval disaster that they have ever faced. I sincerely wish for them to recover as soon as possible.

In addition, I would like to express my thanks to my friends. I am indebted to them for their sincere encouragement and help: dear Jinho Lee, a graduate student in UT Austin; Huirang Kang, a graduate student in Princeton University; and Gubong Lim, my group member.

Finally, I would like to thank my mother, Kyeongsun Hwa, and my older brother, Woosuk Ryu, for their unconditional love and immeasurable support.

# TABLE OF CONTENTS

<b>LIST OF FIGURES</b> . . . . .	<b>vii</b>
<b>LIST OF TABLES</b> . . . . .	<b>x</b>
<b>ABSTRACT</b> . . . . .	<b>xi</b>
 <b>Chapter</b>	
<b>1 INTRODUCTION</b> . . . . .	<b>1</b>
1.1 Background and Motivation . . . . .	1
1.2 Thesis Outline . . . . .	3
1.3 Notations and Abbreviations . . . . .	3
 <b>2 FEMTOCELLULAR ENVIRONMENTS</b> . . . . .	 <b>5</b>
2.1 Network Architecture . . . . .	5
2.2 Technical Challenges . . . . .	6
2.3 Radio Environment . . . . .	8
2.3.1 Path Loss . . . . .	8
2.3.2 Shadow Fading . . . . .	9
2.3.3 Practical Path Loss Models . . . . .	9
2.3.3.1 Outdoor-to-outdoor model . . . . .	10
2.3.3.2 Indoor-to-outdoor model . . . . .	11
2.3.3.3 Indoor-to-indoor model . . . . .	12
2.3.4 Multipath Propagation . . . . .	12
2.3.5 Co-Channel Interference and its management . . . . .	12

<b>3</b>	<b>BEAMFORMING TECHNIQUES</b>	<b>15</b>
3.1	System Overview	15
3.2	TX-BF	16
3.3	TX-BF with Nulling	18
3.3.1	Implementation	18
3.3.2	Beamforming Weights	19
3.4	Codebook-Based BF (CB-BF)	20
<b>4</b>	<b>BEAMFORMING IMPLEMENTATIONS</b>	<b>22</b>
4.1	Assumptions	22
4.2	TX-BF	23
4.3	TX-BF with Nulling	24
4.4	Codebook-Based BF (CB-BF)	26
4.5	Cooperative Transmission	27
<b>5</b>	<b>PERFORMANCE ANALYSIS</b>	<b>30</b>
5.1	The Impact of Different Beamforming Techniques	30
5.1.1	Macro-User Downlink	31
5.1.2	Femto-User Downlink	34
5.2	The Impact of Different Numbers of Femtocells	36
5.3	The Impact of Different Numbers of Antennas	38
5.4	Codebook-Based Beamforming (CB-BF)	40
5.4.1	No PMI Restriction	40
5.4.2	PMI Restriction	41
5.5	The Performance of Cooperative Transmission	44
5.5.1	The Impact of Cooperative Transmission	44
5.5.2	The Impact of Cell Occupancy	47
<b>6</b>	<b>CONCLUSIONS AND FUTURE WORKS</b>	<b>50</b>

BIBLIOGRAPHY . . . . . 52

## LIST OF FIGURES

<b>2.1</b>	Architecture of femtocells . . . . .	6
<b>2.2</b>	Path-loss models for femtocellular environments . . . . .	10
<b>2.3</b>	Co-channel interference scenarios . . . . .	13
<b>3.1</b>	MIMO channel with beamforming . . . . .	16
<b>3.2</b>	TX-BF with nulling . . . . .	18
<b>4.1</b>	Cooperative transmission . . . . .	28
<b>5.1</b>	Comparison of spectral efficiency . . . . .	31
<b>5.2</b>	The CCDF for MUE when 40 FBSs (a) SINR (b) SE . . . . .	32
<b>5.3</b>	The CCDF for MUE when 50 FBSs (a) SINR (b) SE . . . . .	32
<b>5.4</b>	The CCDF for MUE when 40 FBSs (a) SINR (b) SE . . . . .	33
<b>5.5</b>	The CCDF for MUE when 50 FBSs (a) SINR (b) SE . . . . .	33
<b>5.6</b>	The CCDF for FUE when 40 FBSs (a) SINR (b) SE . . . . .	34
<b>5.7</b>	The CCDF for FUE when 50 FBSs (a) SINR (b) SE . . . . .	34
<b>5.8</b>	The CCDF for FUE when 40 FBSs (a) SINR (b) SE . . . . .	35
<b>5.9</b>	The CCDF for FUE when 50 FBSs (a) SINR (b) SE . . . . .	35
<b>5.10</b>	The SE of MUE with different BF techniques (a) 50% (b) 10% . . . . .	36
<b>5.11</b>	The SE of MUE with different nulls (a) 50% (b) 10% . . . . .	37

<b>5.12</b>	The SE of FUE with different BF techniques (a) 50% (b) 10%	37
<b>5.13</b>	The SE of FUE with different nulls (a) 50% (b) 10%	38
<b>5.14</b>	The SE of MUE with different numbers of antennas (a) 50% (b) 10%	39
<b>5.15</b>	The CCDF of total interference for 2 and 4 antennas (a) 40 FBSs (b) 50 FBSs	39
<b>5.16</b>	The SE of FUE with different numbers of antennas (a) 50% (b) 10%	40
<b>5.17</b>	The MUE performance of CB-BF (a) 50% (b) 10%	40
<b>5.18</b>	The FUE performance of CB-BF (a) 50% (b) 10%	41
<b>5.19</b>	The MUE performance of 3-bit CB-BF with PMI restriction (a) 50% (b) 10%	42
<b>5.20</b>	The FUE performance of 3-bit CB-BF with PMI restriction (a) 50% (b) 10%	42
<b>5.21</b>	The MUE performance of 6-bit CB-BF with PMI restriction (a) 50% (b) 10%	43
<b>5.22</b>	The FUE performance of 6-bit CB-BF with PMI restriction (a) 50% (b) 10%	43
<b>5.23</b>	The Poisson distribution with $X = 0$ as a function of $\lambda$	44
<b>5.24</b>	Femtocell group for cooperative transmission	45
<b>5.25</b>	The FUE performance of cooperative transmission (a) 50% (b) 10%	45
<b>5.26</b>	The MUE performance of cooperative transmission (a) 50% (b) 10%	46
<b>5.27</b>	The FUE performances as a function of the probability of idle FBS (a) 50% (b) 10%	47
<b>5.28</b>	The MUE performances as a function of the probability of idle FBS (a) 50% (b) 10%	48

<b>5.29</b>	The FUE performances as a function of the probability of idle FBS (a) 50% (b) 10% . . . . .	48
<b>5.30</b>	The MUE performances as a function of the probability of idle FBS (a) 50% (b) 10% . . . . .	49

## LIST OF TABLES

<b>2.1</b>	Technical challenges of the femtocells . . . . .	7
<b>2.2</b>	Typical path-loss exponents . . . . .	9
<b>3.1</b>	Parameters for codebooks . . . . .	21
<b>4.1</b>	Various pilots in a MIMO system . . . . .	23
<b>4.2</b>	Timing diagram for TX-BF . . . . .	23
<b>4.3</b>	Timing diagram for TX-BF with nulling at MUE . . . . .	24
<b>4.4</b>	Timing diagram for TX-BF with several nulls . . . . .	25
<b>4.5</b>	Timing diagram of CB-BF with no PMI restriction . . . . .	26
<b>4.6</b>	Timing diagram for cooperative transmission . . . . .	29
<b>5.1</b>	Basic parameters for BS . . . . .	30

## ABSTRACT

In recent wireless applications, the demand for higher data rates has dramatically increased, and over 70% of mobile traffic is generated by indoor users. The deployment of femtocells could be one promising solution to this demand. The objective in using femtocells is to expand wireless coverage for indoor users with low-power consumption. In this thesis, we study and analyze the impact of MIMO beamforming schemes in a femtocellular environment. Specifically, we consider a variety of beamforming techniques such as transmit beamforming (TX-BF), transmit beamforming with nulling (TX-BF with nulling), and codebook-based beamforming (CB-BF). We apply these techniques to the femtocellular environment and compare the performance of each technique.

When each femtocellular base station (FBS) employs multiple antennas, beamforming can greatly improve the femtocellular user equipment (FUE) performance, regardless of the number of femtocells. Since the FBSs are installed in the existing macrocell, a technique that protects the macrocellular user equipment (MUE) is required. In this light, TX-BF with nulling at the MUE can obtain the best performance for the FUE while minimizing the interference to the MUE. CB-BF also can be used for each FBS to reduce the computational complexity. This technique can achieve good performance from the FUE point of view, but the MUE performance is not significantly improved until half of all the codewords are restricted. Furthermore, as the number of precoding matrix index (PMI) restriction increases to protect the MUE, the FUE performance degrades. In addition, we have proposed using cooperative transmission among femtocells to improve the FUE and

MUE performance at the same time. Specifically, in a high-density femtocellular environment, this technique might be useful. In reality, however, it is hard to form the cooperative group since the use of femtocells is more likely for personal applications.

# Chapter 1

## INTRODUCTION

### 1.1 Background and Motivation

As wireless applications have moved from voice-only to multimedia data, the demand for higher data rates has dramatically increased. For example, global mobile data traffic surpassed 1.3 *Exabytes* (*EB*, or  $10^{18}$  bytes = *one billion Gigabytes*) in 2008. By 2014, it is estimated that 1.6 *EB* of mobile data will be sent and received each month [1]. Currently, 70-80 percent of the mobile data traffic is generated by indoor users. With the trend to higher and higher rates, cellular operators face a new challenge: how to reliably provide these services to indoor users.

The signal strength, however, for indoor users is significantly degraded by the normal physical structures in a macrocell environment. One way to address this impairment is to install small, low power, access points inside buildings and houses. The use of femtocells, as these small cells are called [2], is one of the most promising solutions to increase coverage and capacity. Femtocells are user-deployed and operate in licensed spectrum to connect a standard mobile device to a mobile operator's network using residential *digital subscriber line* (DSL) or cable broadband connections [2]. The installation of many femtocells in a macrocell also creates several new challenges, especially in terms of the interference to macrocellular users. Many of these issues have been addressed; some preliminary ideas are presented in [3]. Interference management and performance analysis, particularly, have been studied in [4]-[5].

State-of-the-art techniques in wireless communication, such as *multiple-input multiple-output* (MIMO) beamforming, can be applied to minimize the interference problem caused by the introduction of femtocells. The use of multiple antennas at both ends of the wireless link is an effective way to improve performance [6]-[8]. In an *independent and identically distributed* (i.i.d) Rayleigh fading environment, the channel capacity increases with the number of transmit and receive antennas [6]-[7]. In cellular systems, especially, it is shown that a MIMO system can achieve a substantial increase in spectral efficiency ( $b/s/Hz$ ) in single-cell environments [9]-[10]. In multi-cell environments, however, the *co-channel interferences* (CCI) from adjacent cells severely degrades the performances [11]-[12]. Therefore, to realize the potential benefits of the deployment of femtocells, effective interference management techniques are required to improve the *signal-to-interference-plus-noise ratio* (SINR).

It is well known that beamforming at the transmitter can improve the performance by exploiting *channel state information* (CSI). In *transmit beamforming* (TX-BF), the transmit power is directed toward the receiver to maximize the *signal-to-noise ratio* (SNR) [7]. The performance analysis in terms of the outage probability and ergodic capacity have been studied in [13]. In the presence of CCI, TX-BF is not always the best approach. One transmitter-based approach for mitigating CCI is to create a null in the direction of other users. This is called *transmit beamforming with nulling* (TX-BF with nulling), and is proposed in [14]. In TX-BF with nulling, the goals are to maximize the signal power to the receiver and minimize the interference to users served by other base stations. Both TX-BF and TX-BF with nulling increase the computational complexity and require accurate and timely feedback to achieve the best performance.

*Codebook-based beamforming* (CB-BF), studied in [15]-[18], can reduce the computational complexity of TX-BF techniques, and the use of a *pre-coding matrix*

*index* (PMI) with restrictions can reduce interference. This approach has been proposed in the downlink for cell-edge users [19]. This scheme restricts the usage of codebook subsets at the transmitter, based on the strongest interference at the receiver to minimize interference.

In this thesis, we will analyze the downlink performance for both the macrocellular and femtocellular users. Several beamforming techniques will be applied in each femtocell. Different scenarios will be investigated using single macrocell with different numbers of femtocells.

## 1.2 Thesis Outline

The rest of the thesis is structured as follows: An overview of the femtocellular environment will be presented in Chapter 2. In Chapter 3, we review several beamforming techniques. Specifically, we concentrate on beamforming with nulling and PMI. The adopted algorithms and the scenarios will be presented in Chapter 4. A new scheme, based on cooperation among femtocells, will also be presented in Chapter 4. In Chapter 5, we present simulation results and analyze the performance of the various beamforming techniques. Finally, we present our conclusions and discuss future work in Chapter 6.

## 1.3 Notations and Abbreviations

In this paper, plain letters such as  $a$  and  $A$  represent scalar values and bold-face letters, for example,  $\mathbf{a}$  and  $\mathbf{A}$ , represent vectors or matrices. We also use the following notations and abbreviations:

$E[\mathbf{X}]$	Expected value of $\mathbf{X}$
$\ \mathbf{a}\ $	Euclidean norm of vector $\mathbf{a}$
$ \mathbf{a} $	Absolute value of $\mathbf{a}$
$\mathbf{A}^\dagger$	Hermitian matrix of $\mathbf{A}$
$\mathbf{A}^*$	Conjugate transpose of $\mathbf{A}$

BS	Base Station
CCI	Co-Channel Interference
CCDF	Complementary Cumulative Distribution Function
CDF	Cumulative Distribution Function
CSI	Channel State Information
FDD	Frequency Division Duplexing
FBS	Femtocellular Base Station
FUE	Femtocellular User Equipment
i.i.d	Independent and Identically Distributed
ISP	Internet Service Provider
LOS	Line of Sight
MIMO	Multiple-Input Multiple-Output
MBS	Macrocellular Base Station
MUE	Macrocellular User Equipment
NLOS	Non-Line of Sight
PSTN	Public Switched Telephone Network
QoS	Quality of Service
SINR	Signal-to-Interference-plus-Noise Ratio
SNR	Signal-to-Noise Ratio
SE	Spectral Efficiency
SVD	Singular-Value Decomposition
TDD	Time Division Duplexing

## Chapter 2

### FEMTOCELLULAR ENVIRONMENTS

Femtocells will be deployed in existing cellular systems, and will use the same pool of resources. Ideally, the addition of a femtocell in a home, for example, should be as simple as installing a Wi-Fi access point. With this goal in mind, the deployment of femtocell faces several technical challenges. In this chapter, we describe the femtocellular architecture and the characteristics of the radio environment.

#### 2.1 Network Architecture

Standards organizations, such as the Third Generation Partnership Project (3GPP), 3GPP2, and WiMAX Forum, are developing solutions for their individual target applications [20]-[22]. So, as expected, each also has their own approach for the commercial introduction of femtocells. In general though, the applications for femtocells fall into two broad categories: public access and home or enterprise femtocells [23].

The basic architecture is a hierarchical one, and is shown in Fig. 2.1. All of the FBSs are connected to the local ISP networks to reduce the cost of the backbone installation. Through the backbone networks, each femtocell can communicate with the cellular operators as well as the PSTN. Since the FBSs are user-deployed, the number of femtocells cannot be planned in advance by the cellular operators, making it difficult to manage the femtocellular networks after they have been deployed. There are numerous technical and economic challenges in effectively deploying femtocells [3]. Here, we concentrate on the technical issues.

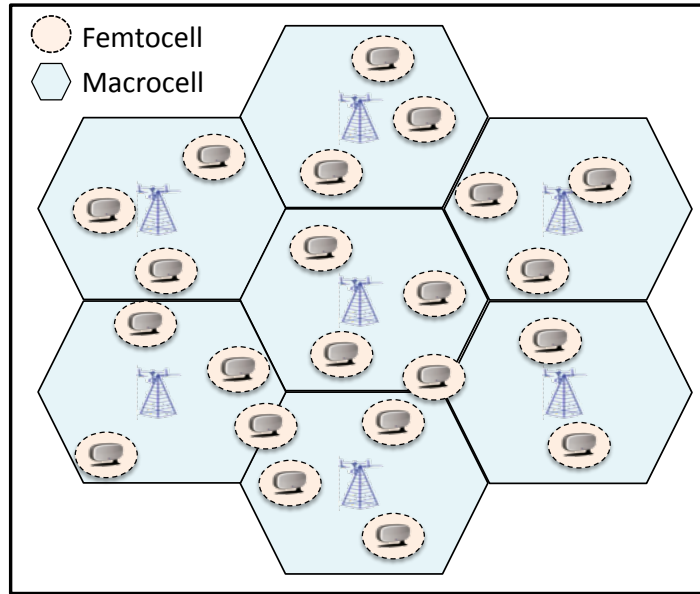


**Figure 2.1:** Architecture of femtocells

## 2.2 Technical Challenges

There are several technical challenges to overcome if femtocells are to be deployed effectively [3]. First and foremost, CCI increases as the number of femtocells increases. The maximum channel capacity is given by Shannon's classic formula, relating bandwidth  $W$   $Hz$  and  $SNR$  [24]

$$C = W \log_2(1 + SNR) \quad (2.1)$$

For a given bandwidth, then, the capacity can be improved by increasing the SNR or, for a cellular system, increasing the  $SINR$ , the ratio of the received signal power and the sum of the powers of the interference from other cells and the thermal noise. Clearly, in general, the maximum channel capacity will be lower when femtocells are deployed unless careful attention is paid to minimizing this interference.

Typically, there are three sources of CCI: 1) macrocell to femtocell, 2) femtocell to femtocell, and 3) femtocell to macrocell. Due to the low transmit power of femtocells, 1) and 3) are the main sources that need to be considered. Since

femtocells are installed by the end-users, it is especially difficult to plan the frequency allocation for each femtocell to avoid CCI. Therefore, other approaches to interference mitigation are required.

The deployment of femtocells requires synchronization to help minimize the multi-access interference, and to ensure a tolerable carrier offset. Synchronization is also required to handoff from macrocell user to a femtocell, or vice versa. Specifically, in a TDD system, an accurate reference is required for coordinating the absolute phases for forward and reverse transmission. To solve those problems, efficient synchronization methods have been considered, such as the *IEEE-1588 precision timing protocol over IP* (potential timing accuracy of 100 ns) or the *self-adaptive timing recovery protocol* [3]. Furthermore, femtocells equipped with GPS are also being considered for maintaining stable indoor satellite reception.

Since each femtocell is connected to the Internet backbone, the backhaul link must have sufficient capacity to avoid a traffic bottleneck. The current Internet backbone, however, is not equipped to provide the delay resiliency. Therefore, both the ISP company and the cellular company have to maintain a tight relationship when their services are independently offered to the end-user.

Technical Challenges	Descriptions
CCI	Macro-User - Interference from Femtocells Femto-User - Interference from Macrocell - Interference from other Femtocells
Synchronization	Multi-access interference Handoff between MBS and FBS
QoS	Guarantee sufficient capacity in Internet backbone

**Table 2.1:** Technical challenges of the femtocells

Table 2.1 summarizes the technical challenges. Next, we review the characteristics of the cellular radio environment.

## 2.3 Radio Environment

The wireless channel is characterized by the path loss between the transmitter and receiver. The signal attenuation caused by obstructions, multipath fading, and co-channel interference resulting from reusing the system resources. In this section, we describe the models used for path loss, shadow fading, and Rayleigh fading.

### 2.3.1 Path Loss

The path loss is defined as the ratio of the received power and the transmitted power. There are various path-loss models for cellular environments. We consider first a simple path-loss model, called the free-space model. In this model, there are no scatterers, not even the ground, and we assume Line-Of-Sight (LOS) transmission. The free-space path-loss model is given by [25]

$$PL = \frac{P_r}{P_t} = \left[ \frac{\sqrt{G_t}\lambda}{4\pi d} \right]^2 \quad (2.2)$$

where  $P_t$  and  $P_r$  is the transmitted and the received power, respectively.  $\sqrt{G_t}$  represents the product of the transmit and receive antenna field radiation patterns in the LOS direction,  $\lambda$  is the wavelength of the propagating signal, and  $d$  is the distance between the transmitter and the receiver.

In a typical mobile environment, especially urban and indoor, a transmitted signal scatters off objects, introducing reflection and diffraction. As a result, the received signal is actually the sum of multiple versions of the transmitted signal, each with different phases, amplitudes, and times of arrival. To account for the large-scale effects of these scatters, we consider the following

$$PL = \frac{P_r}{P_t} = \left( \frac{\lambda}{4\pi d_0} \right)^2 \left[ \frac{d_0}{d} \right]^\gamma \quad (2.3)$$

where  $d_0$  is a reference distance for the antenna far field, and  $\gamma$  is the path-loss exponent. The values of these two components are usually obtained empirically through measurements. Typically,  $d_0$  is assumed to be 1 to 10 *m* for an indoor

environment and 10 to 100  $m$  outdoors. The following table summarizes the typical values of  $\gamma$  for different environments [25].

Environment	$\gamma$ range
Urban macrocells	3.7 – 6.5
Urban microcells	2.7 – 3.5
Office building (same floor)	1.6 – 3.5
Office building (multiple floors)	2 – 6
Store	1.8 – 2.2
Factory	1.6 – 3.3
Home	3

**Table 2.2:** Typical path-loss exponents

### 2.3.2 Shadow Fading

A transmitted signal could also be blocked by obstacles such as trees and buildings and even people. This phenomenon, so-called shadowing, can severely reduce the signal strength. Due to the random nature of this impairment in mobile environments, statistical models are used to characterize it. The best-known model, called *log normal shadowing*, assumes that the signal strength, in decibels ( $dB$ ), is Gaussian that is [25]

$$p(s) = \frac{1}{\sqrt{2\pi\sigma_s^2}} \exp\left[-\frac{(s - \bar{s})^2}{2\sigma_s^2}\right] \quad (2.4)$$

where  $p(\bullet)$  is the probability density function of the signal strength  $s$  in  $dB$  and  $\bar{s}$  and  $\sigma_s^2$  are the mean and the variance of  $s$  in  $dB$ , respectively.

### 2.3.3 Practical Path Loss Models

To more accurately determine the performance of femtocellular systems, we will consider instead three path-loss models that have been suggested from empirical studies for standards' activities [26]-[28]: outdoor-to-outdoor (outdoor-to-indoor), indoor-to-outdoor, and indoor-to-indoor. The three scenarios are illustrated in Fig. 2.2.

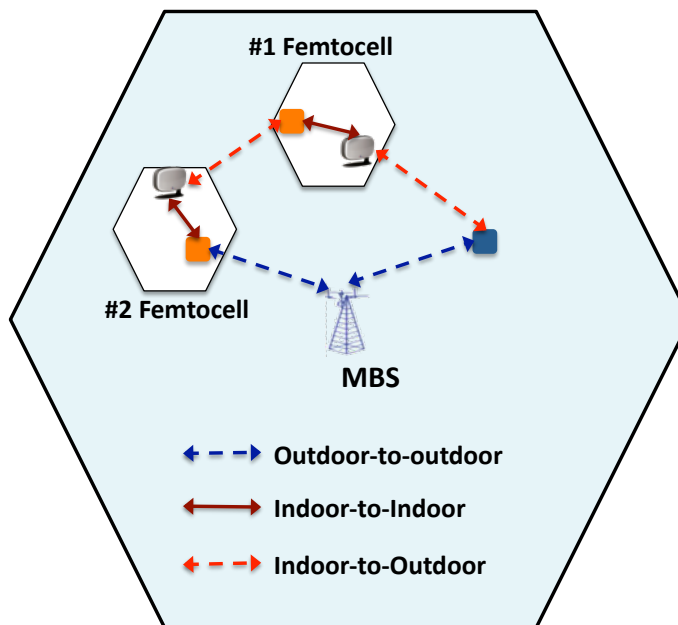


**Figure 2.2:** Path-loss models for femtocellular environments

### 2.3.3.1 Outdoor-to-outdoor model

This path-loss model can be applied to the channel between the MBS and the MUE, or vice versa. It also can be utilized for the FUE with additional wall losses (outdoor-to-indoor). The additional losses can be modeled as 12 *dB* for a heavy wall and 5 *dB* for a light wall [26]. The assumptions for this path-loss model are that the BS has a high transmit power and the environment is NLOS. The path loss in this case can be represented as

$$PL(dB) = 40(1 - 4 \times 10^{-3} \Delta h_b) \log_{10} d - 18 \log_{10} \Delta h_b + 21 \log_{10} f_c + 80 \quad (2.5)$$

where  $d$  is the distance between the BS and the MS (*km*),  $f_c$  is the carrier frequency (*MHz*), and  $\Delta h_b$  is the antenna height (*m*) measured from the average rooftop level. The mean of the building penetration loss is 12 *dB* and the standard deviation for the shadow fading is assumed to be 10 *dB*.

### 2.3.3.2 Indoor-to-outdoor model

This model can be applied to the link between the FBS and the outdoor MUE, or vice versa. Furthermore, this path-loss model, with additional wall loss, is also applicable to the link between the FBS and other FUEs which are located in other femtocells. This model can be expressed as [27]

$$PL(dB) = PL_b + PL_{tw} + PL_{in} \quad (2.6)$$

where  $PL_b$  is the path loss between the FBS and the outdoor MUE.  $PL_{tw}$  is the exterior wall penetration loss, and  $PL_{in}$  is the path loss from the FBS to the nearest wall. Specifically,

$$PL_b = \max(PL_{B1}, P_{free}) \quad (2.7)$$

$$PL_{B1} = 41 + 20 \log_{10}(f_c/5) + 22.7 \log_{10}(d_{out} + d_{in}) \quad (2.8)$$

$$PL_{free} = 20 \log_{10} d + 46.4 + 20 \log_{10}(f_c/5) \quad (2.9)$$

where  $PL_{B1}$  is an urban microcell scenario and  $PL_{free}$  is the free-space path loss [26][28]. For (2.6)-(2.9), the carrier frequency  $f_c$  is in *GHz*, and  $d$  is the distance between the FBS and the MUE or other FUEs.  $d_{out}$  is the distance between the outdoor path and the wall, and  $d_{in}$  is the distance from the FBS to the nearest point of the wall. Normally, the direct distance from the FBS and MUE or FUE,  $d$ , is the sum of  $d_{out}$  and  $d_{in}$ . The second term in (2.6) can be expressed as

$$PL_{tw} = 14 + 15(1 - \cos \theta)^2 \quad (2.10)$$

where  $\theta$  is the angle between the outdoor path and the wall. The final term in (2.6) is

$$PL_{in} = 0.5d_{in} \quad (2.11)$$

### 2.3.3.3 Indoor-to-indoor model

This model for the channel between the FBS and its FUE can be represented by [28]

$$PL(dB) = 37 + 30 \log_{10} d + 18.3n \frac{n+2}{n+1} - 0.46 \quad (2.12)$$

where  $n$  is the number of floors in the path. The standard deviation of the model is 12  $dB$  and no wall loss is included in this model.

### 2.3.4 Multipath Propagation

In addition to the average path loss and shadow, there is an additional component to the signal attenuation caused by the constructive and destructive addition of the multiple paths from the transmitter to the receiver. This is called multipath fading [25]. When the number of scatterers is large, the resulting signal amplitude can be represented by a *Rayleigh distribution*

$$p(r) = \frac{r}{\sigma^2} \exp\left[-\frac{r^2}{2\sigma^2}\right] \quad (2.13)$$

where  $r$  is the envelope of received signal and  $2\sigma^2$  is the mean power of the multipath signal. Fading can severely degrade the performance of a wireless system. Multiple antennas can be utilized at the transmitter or receiver to improve the performance.

### 2.3.5 Co-Channel Interference and its management

Bandwidth is a precious resource in wireless communications. To most efficiently utilize the spectrum in a cellular system, frequencies are reused resulting in co-channel interference (CCI). Femtocellular networks are hierarchical systems and, as such, CCI must be efficiently managed. Since the objective is to have femtocells deployed by individual users, MUE might experience significant CCI when a large number of femtocells are deployed in a macrocell. On the other hand, the FUE will not be as severely affected because it is relatively close to its own FBS. A typical scenario is shown in Fig. 2.3. Clearly, the management of CCI, especially

to the MUE, is a critical issue for the introduction of femtocells into an existing macrocellular system.

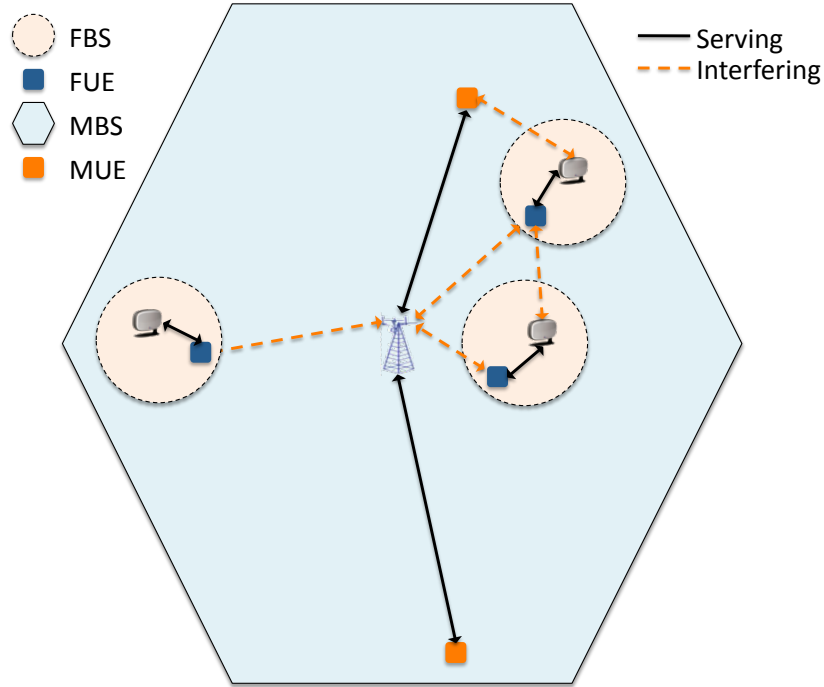


**Figure 2.3:** Co-channel interference scenarios

In this thesis, we mainly focus on interference management for the down-link.(that is, base-to-mobile direction).

- Interference to MUEs:

The users who are served by the MBS could be located anywhere in their serving macrocell. In this case, there are two sources of interference: MBSs in adjacent cells and FBSs. The MUEs located at the cell edge could have significant levels of CCI from adjacent cells and their distance from their serving MBS makes them even more vulnerable to interference from FBSs. Obviously, as the number of femtocells increases, on average, the CCI will also increase. Therefore, a strategy for protecting the MUE is required when femtocells are deployed.

- Interference to FUEs:

Users who are communicating with the FBS will most often be located inside a building or house and will not be mobile. In this case, the major source of interference is the MBS. The closer the femtocells are placed to the MBS, the greater the CCI. In addition, when the femtocells are located at the edge of a macrocell, the interference from adjacent macrocells could also be significant. Finally, the FUE will also suffer from interference from other FBSs. In general, this interference is relatively low due to the lower transmit power of the FBSs. However, when the distance between the femtocells is short enough, this interference must be taken into account.

The goal of the work described in this thesis is to develop algorithms to deploy femtocells with the least disturbance to the macrocellular users, while guaranteeing some level of service to femtocellular users. In particular, we will focus on beamforming as a method of interference mitigation.

## Chapter 3

# BEAMFORMING TECHNIQUES

Beamforming is a promising technique for improving the received signal strength and mitigating co-channel interference. In this chapter, we describe three MIMO beamforming techniques: transmit beamforming (TX-BF) [7], transmit beamforming with nulling (TX-BF with nulling) [14], and codebook-based beamforming (CB-BF) [18]-[19].

### 3.1 System Overview

In the general form of a MIMO system, both the transmitter and the receiver have multiple antennas. The system model, assuming only a single data stream ( $N_s = 1$ ), can be represented as

$$\mathbf{y} = p\mathbf{H}\mathbf{x} + \mathbf{n} \quad (3.1)$$

where  $p$  is the average received power and  $\mathbf{H}$  is an  $(N_r \times N_t)$  channel gain matrix.  $N_r$  and  $N_t$  denote the number of receive and transmit antennas, respectively.  $\mathbf{y}$  is the received signal vector (of length  $N_r$ ) and  $\mathbf{x}$  is the transmitted vector (of length  $N_t$ ). The last term in (3.1) is additive noise which is modeled as white and Gaussian.

In beamforming, the same symbol,  $x$ , is sent over each transmit antenna. This means that the input covariance matrix has unit rank [25]. This scheme includes a precoding vector  $\mathbf{q}$  at the transmitter (of length  $N_t$ ), and a shaping vector  $\mathbf{u}$  at the receiver (of length  $N_r$ ), as shown in Fig. 3.1. Thus, (3.1) can be modified as

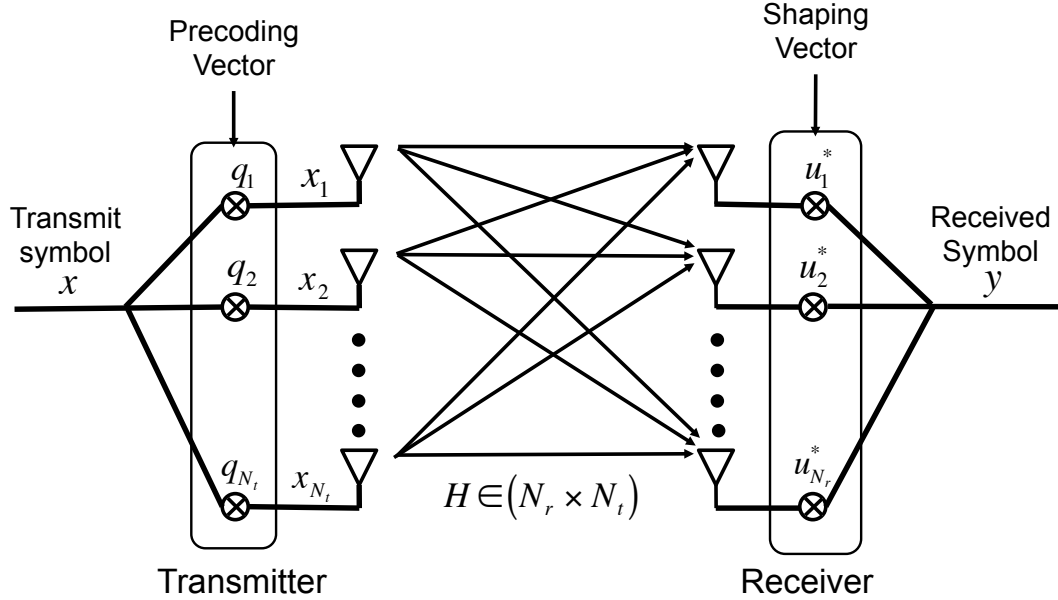


**Figure 3.1:** MIMO channel with beamforming

$$y = \mathbf{p}\mathbf{u}^\dagger\mathbf{H}\mathbf{q}x + \mathbf{u}^\dagger\mathbf{n} \quad (3.2)$$

where  $x$  is the transmitted signal and  $\mathbf{u}^\dagger$  represents the *Hermitian* of  $\mathbf{u}$ . If the components of  $\mathbf{n}$  are independent and identically distributed, then the statistics of  $\mathbf{u}^\dagger\mathbf{n}$  are the same as the statistics for each of these components. Both the transmit and receive weight vectors are normalized so that  $\|\mathbf{u}\| = \|\mathbf{q}\| = 1$ . Here, we assume that there is one antenna at the receiver; then, the shaping vector  $\mathbf{u}$  can be ignored.

### 3.2 TX-BF

Conceptually, in TX-BF, the objective is to put a beam in the direction to the desired user to maximize the signal power. Assume that the channel gain matrix  $\mathbf{H}$  is known. Then, the optimal beamforming weights at the transmitter can be obtained using a singular value decomposition (SVD) of  $\mathbf{H}$  [7]

$$\mathbf{H} = \mathbf{U}\mathbf{\Sigma}\mathbf{V}^\dagger \quad (3.3)$$

where  $\mathbf{U}$  and  $\mathbf{V}$  are unitary matrices of size  $(N_r \times N_r)$  and  $(N_t \times N_t)$ , respectively, and  $\mathbf{\Sigma}$  is an  $(N_r \times N_t)$  diagonal matrix with singular values  $\sigma_i$ . The singular value  $\sigma_i$  is equal to  $\sqrt{\lambda_i}$ , where  $\lambda_i$  is the largest eigenvalue of  $\mathbf{H}\mathbf{H}^\dagger$ . The beamforming weights correspond to the largest singular value of channel  $\mathbf{H}$ , so that the first column vector of the singular vector  $\mathbf{V}$  is used for the beamforming weights.

We consider a multi-cell environment with  $J$  cells surrounding the desired cell/user. Assume that each cell has its own user, resulting in  $J$  users uniformly distributed within their cell's coverage area. We also assume that each user device employs only one receive antenna, so the channel gain matrix reduces to a vector  $\mathbf{h}$  of length  $N_t$ . Each BS performs TX-BF independently. The received signal at the desired user can then be expressed as

$$y = \underbrace{p\mathbf{h}\mathbf{w}x}_{\text{desired signal}} + \underbrace{\sum_{j=1}^J p_j \mathbf{h}_j \mathbf{w}_j x_j}_{\text{interfered signal}} + \mathbf{n} \quad (3.4)$$

where  $p$  is the average received power and  $\mathbf{w}$  denotes the TX-BF weights for a given base station. Since the coefficients of the channel gain vector  $\mathbf{h}$  are modeled as i.i.d. complex Gaussian random variables with zero-mean and unit variance, the SINR for the desired user is given by

$$SINR = \frac{p|\mathbf{h}\mathbf{w}|^2}{\sum_j p_j |\mathbf{h}_j \mathbf{w}_j|^2 + p_N} \quad (3.5)$$

when no receiver processing is performed ( $N_r = 1$ ). The last term of the denominator is the additive noise power.

TX-BF can maximize the signal power to the desired user. In a single-user, single-cell environment, TX-BF can maximize performance. When there are multiple users, this approach is not best because no attempt is made to minimize the interference to other users.

### 3.3 TX-BF with Nulling

In TX-BF with nulling, the BS performs TX-BF to the desired user and puts a null in the direction of the unintended user(s) to minimize the interference. This

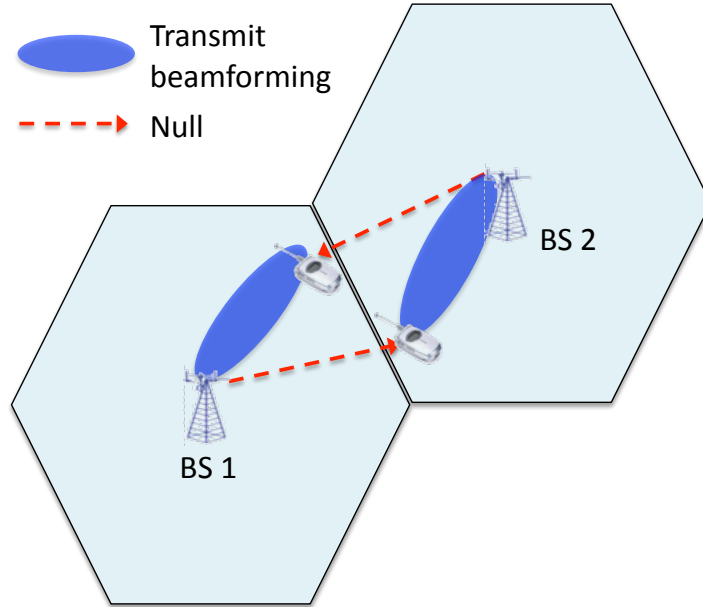


**Figure 3.2:** TX-BF with nulling

technique has been proposed to increase the SINR of the cell-edge user by reducing interference from other BSs [14], as shown in Fig. 3.2. Therefore, the desired MS can achieve the maximum SINR by TX-BF from the serving BS and nulling from other BSs. Imperfect knowledge of the interference statistics and a limited number of transmit antennas at BS can limit the ability to achieve the maximum SINR. Also, to implement this approach, feedback is increased and the delay between the BS and MS could cause additional degradation in performance.

#### 3.3.1 Implementation

We assume all BSs are connected to each other via a backhaul network for sharing CSI. Each MS measures the desired CSI ( $H_d$ ) from the serving BS and the

interfering BSs ( $H_i$ ). These measurements are sent to the BSs; then, the BS chooses the desired user in a time slot and this scheduling information is shared among all BSs of interest. At the same time, the BS also measures the interference powers. Based on this information, each BS selects the MSs for nulling. The number of null beams that the BS can create is based on the number of transmit antennas. For example, if there are four antennas ( $N_t = 4$ ) at the BS, then the maximum number of nulls is three ( $N_t - 1$ ).

### 3.3.2 Beamforming Weights

Assume that there are  $J$  co-channel cells around the desired cell, and only one receive antenna is used. As discussed above, TX-BF with nulling maximizes the average signal power to the desired user and minimizes the average signal power received by the co-channel users. The transmit weight vectors  $\mathbf{w}^{opt}$  can be calculated using these two criteria. The average signal power to the desired user is

$$E[|\mathbf{h}\mathbf{w}|^2] = E[\mathbf{w}^\dagger \mathbf{h}^\dagger \mathbf{h} \mathbf{w}] = \mathbf{w}^\dagger \mathbf{R} \mathbf{w} \quad (3.6)$$

where  $\mathbf{h}$  is the channel gain vector (of length  $N_t$ ) for a desired user and  $\mathbf{R}$  is correlation matrix of  $E[\mathbf{h}^\dagger \mathbf{h}]$ . The average interference power from  $J$  co-channel cells can be expressed as

$$\sum_{j=1}^J E[|\mathbf{h}_j \mathbf{w}|^2] = \sum_{j=1}^J E[\mathbf{w}^\dagger \mathbf{h}_j^\dagger \mathbf{h}_j \mathbf{w}] = \sum_{j=1}^J \mathbf{w}^\dagger \mathbf{R}_j \mathbf{w} \quad (3.7)$$

where  $\mathbf{h}_j$  is channel gain vector (of length  $N_t$ ) from the  $J$  co-channel cells to the desired user.  $\mathbf{R}_j$  is the covariance matrix  $E[\mathbf{h}_j^\dagger \mathbf{h}_j]$ .

With these two components, the optimal beamforming weights at the desired BS can then be obtained by the following optimization problem [30]

$$\mathbf{w}^{opt} = \arg \max_{\|\mathbf{w}\|=1} \frac{\mathbf{w}^\dagger \mathbf{R} \mathbf{w}}{\sum_j \mathbf{w}^\dagger \mathbf{R}_j \mathbf{w} + p_N} \quad (3.8)$$

which can be solved as

$$\mathbf{w}^{opt} = \mathbf{V} \left[ \left( \sum_{j=1}^J \mathbf{R}_j + p_N I_N \right)^{-1} \mathbf{R} \right] \quad (3.9)$$

where  $\mathbf{V}[\mathbf{X}]$  denotes the eigenvector corresponding to the largest eigenvalue of  $\mathbf{X}$ .  $p_N$  is the noise power and  $I_N$  is an  $(N_t \times N_t)$  identity matrix.

### 3.4 Codebook-Based BF (CB-BF)

The CB-BF is used for a closed-loop environment, similar to TX-BF or TX-BF with nulling. The difference is that the beamforming vectors are not calculated at each BS to reduce the computational complexity and feedback delay; but rather are stored in each BS's memory in advance. In [18], two codebook sets for four antennas are suggested with 3-bit and 6-bit feedback sizes. We will utilize this method of codebook generation, and apply it to our femtocellular environment.

The codebook is specified by the first codeword  $\mathbf{W}_1$  and a diagonal rotation matrix  $\mathbf{G}$  [18] such that

$$\mathbf{W}_l = \mathbf{G}^{l-1} \mathbf{W}_1 \quad (3.10)$$

for  $l = 2, 3, \dots, 2^L$ . Each codeword is of length  $N_t$  and the rotation matrix  $\mathbf{G} = \text{diag}[e^{j\frac{2\pi}{2^L}u_1}, \dots, e^{j\frac{2\pi}{2^L}u_{N_t}}]$  where  $L$  is the number of bits per feedback and  $\mathbf{u}$  is an integer vector of length  $N_t$ . Furthermore,  $\mathbf{W}_1$  is chosen to be an  $N_t \times 1$  submatrix of the  $(N_t \times N_t)$  DFT matrix  $\mathbf{F}$ , whose entry on the  $i$ th row and  $j$ th column is  $e^{j\frac{2\pi}{N_t}(i-1)(j-1)}$ .

Since  $\mathbf{G}$  is diagonal, it can be written as part of an eigen-decomposition

$$\mathbf{S} = \mathbf{M}\mathbf{G}\mathbf{M}^* \quad (3.11)$$

where  $\mathbf{M}$  is an  $(N_t \times N_t)$  unitary matrix, parameterized as

$$\mathbf{M} = \mathbf{I} - 2\mathbf{b}\mathbf{b}^* \quad (3.12)$$

where  $\mathbf{b}$  is an  $(N_t \times 1)$  unit vector. The rotation matrix  $\mathbf{G}$  can be replaced by  $\mathbf{S}$  in (3.15) as

$$\mathbf{W}_l = \mathbf{S}^{l-1} \mathbf{W}_1 = (\mathbf{MGM}^*)^{l-1} \mathbf{W}_1 = \mathbf{MF}^{l-1} \mathbf{M}^* \mathbf{W}_1 \quad (3.13)$$

for  $l = 2, 3, \dots, 2^L$ . Table 3.1 gives parameters for the codebooks [18] and the first codeword  $\mathbf{W}_1$  is chosen to be  $[0.5; 0.5i; -0.5; -0.5i]$ .

$N_t$	$N_s$	$L$	$\mathbf{u}$	$\mathbf{b}$
4	1	3	[1,2,7,6]	$[0.2895 + 0.3635i; 0.5287 - 0.2752i;$ $-0.2352 - 0.4247i; -0.4040 + 0.1729i]$
4	1	6	[1,45,22,49]	$[0.3954 - 0.0738i; 0.0206 + 0.4326i;$ $-0.1658 - 0.5445i; 0.5487 - 0.1599i]$

**Table 3.1:** Parameters for codebooks

## Chapter 4

### BEAMFORMING IMPLEMENTATIONS

Based on the various beamforming techniques, in this chapter, we describe these algorithms for a femtocellular environment. Additionally, a new beamforming algorithm, called cooperative transmission, will be described.

#### 4.1 Assumptions

We assume there is only one mobile user in each BS. The MUE is uniformly distributed in a macrocell and is assumed to move at low speed, less than 10 *km/h*. Likewise, each FUE is also uniformly distributed in its own femtocell. Furthermore, every femtocell is uniformly located in a macrocell. We also assume both the MUE and FUE remain in their serving cell.

Multiple transmit antennas are available in every BS, and each mobile user has only one receive antenna. We consider a TDD system, so the uplink and downlink channel are reciprocal. Therefore, the CSI can be obtained in the uplink or the downlink. Each Rayleigh channel is i.i.d complex Gaussian with zero mean and unit variance.

In a MIMO system, pilots can be used for synchronization (both time and frequency), and for acquisition of CSI. For example, pilot signals in a MIMO system have been described in [32]. We will consider various pilots based on this patent, but we add one more pilot which is a reference pilot from a mobile user to the BS related to the one antenna at the mobile user. The following table summarizes the types of pilots. We can assume a Walsh code is used for the orthogonal codes in the

<b>Types of Pilots</b>	<b>Descriptions</b>
<i>Beacon Pilot</i>	Transmitted from all transmit antennas and used for time and frequency acquisition. Also, the type of BS is included.
<i>MIMO Pilot</i>	Transmitted from all transmit antennas with different orthogonal codes and used for channel estimation.
<i>Steered Reference</i> (BF to User)	Transmitted on specific eigen-modes of a MIMO channel for a specific user and used for channel estimation and possibly rate control.
<i>Reference</i> (User to BF)	Used for channel estimation and identified the MUE and each FUE with different orthogonal codes.
<i>Carrier Pilot</i>	Used for phase tracking of a carrier signal.

**Table 4.1:** Various pilots in a MIMO system

MIMO and reference pilots.

#### 4.2 TX-BF

	<b>FBS</b>	<b>FUE</b>
$t_0$	- Transmits beacon and MIMO pilot on the downlink in each TDD frame.	- Receives beacon and MIMO pilot, and acquires system - Estimate downlink CSI ( $\mathbf{h}_{FUE}^d$ ) based on MIMO pilot.
$t_1$	- Receives reference signal, and obtain downlink CSI ( $\mathbf{h}_{FUE}^d$ ). - Calculates weight vectors ( $\mathbf{w}$ ) by SVD.	- Transmits reference signal.
$t_2$	- Serves its FUE.	- Receives symbols from serving FBS.

**Table 4.2:** Timing diagram for TX-BF

In this case, all of the FBSs perform TX-BF, and the MBS does not perform any beamforming technique. The required CSI to compute the TX-BF weights is the channel between the FBS and the desired FUE ( $\mathbf{h}_{FUE}^d$ ). The TX-BF weights  $\mathbf{w}$  can be obtained by SVD. Table 4.2 is the timing diagram of the TX-BF in a TDD

system. This process is also applied to all of the FBSs which have their own user. As mentioned above, TX-BF can obtain good performance for the desired FUE regardless of the location of other FUEs; however, it can degrade the performance of the other FUEs.

### 4.3 TX-BF with Nulling

This algorithm is similar to the TX-BF case with the additional requirement of creating nulls in the direction of other users. The downlink CSI can be acquired using the MIMO and reference pilots. Furthermore, the MUE and FUE can be identified by the reference pilot since they use orthogonal codes. In this sense, each FBS has both the desired channel for the serving FUE and the interference channels for the MUE or other FUE(s).

	<b>FBS</b>	<b>FUE</b>	<b>MUE</b>
$t_0$	- Transmits beacon and MIMO pilot on downlink in each TDD frame.	- Receives beacon and MIMO pilot, and acquires system. - Estimates downlink CSI( $\mathbf{h}_{FUE}^d$ ) based on MIMO pilot.	- Receives beacon and MIMO pilot, and acquire system. - Estimates downlink CSIs ( $\mathbf{h}_{MUE}^{(i)}$ ) of each FBS based on MIMO. pilot.
$t_1$	- Receives reference signal, and obtain downlink of desired channel ( $\mathbf{h}_{FUE}^d$ ) and interfering channel ( $\mathbf{h}_{MUE}$ ) - Calculates weight vectors ( $\mathbf{w}^{opt}$ )	- Transmits reference signal.	- Transmits reference signal.
$t_2$	- Serves its FUE (TX-BF with nulling)	- Receives symbols from serving FBS	- Receives symbols from serving MBS

**Table 4.3:** Timing diagram for TX-BF with nulling at MUE

With the acquired CSIs, we consider first that every FBS creates a null to the MUE. Each FBS can obtain the optimal weight vectors for the TX-BF with nulling based on the channel to the FUE ( $\mathbf{h}_{FUE}^d$ ) and to the MUE ( $\mathbf{h}_{MUE}$ ). Then, each FBS performs TX-BF for its FUE and puts a null in the direction of the MUE. Table 4.3 describes this process.

	<b>FBS</b>	<b>FUE</b>	<b>MUE</b>
$t_0$	- Transmits beacon and MIMO pilot on downlink in each TDD frame.	- Receives beacon and MIMO pilot, and acquires system. - Estimates downlink CSI of desired FUE ( $\mathbf{h}_{FUE}^d$ ) and other FUE ( $\mathbf{h}_{FUE}^{(i)}$ ) based on MIMO pilot	- Receives beacon and MIMO pilot, and acquires system. - Estimates downlink CSIs ( $\mathbf{h}_{MUE}^{(i)}$ ) of each FBS based on MIMO pilot.
$t_1$	- Receives reference signal and obtain downlink of desired channel ( $\mathbf{h}_{FUE}^d$ ) and interfering channel ( $\mathbf{h}_{MUE}, \mathbf{h}_{MUE}^{(i)}$ ) - Identifies strongest interfering channel of other FUE ( $\max \mathbf{h}_{FUE}^{(i)} ^2$ ) - Calculates weight vectors ( $\mathbf{w}^{opt}$ )	- Transmits reference signal.	- Transmits reference signal.
$t_2$	- Serves its FUE (TX-BF with nulling)	- Receives symbols from serving FBS	- Receives symbols from serving MBS

**Table 4.4:** Timing diagram for TX-BF with several nulls

Here, we also assume that the deployed femtocells can create additional nulls to minimize the interference to other FUEs. The basic process is the same as the TX-BF with nulling at the MUE. The FBS measures the uplink signal strength of each FUE based on the reference pilot. The FBS determines the direction of the

additional nulls based on the strongest uplink signal power for the other FUEs. In the case of 3 nulls, for example, the first null is for the MUE ( $\mathbf{h}_{MUE}$ ), the second null is the FUE ( $\mathbf{h}_{FUE}^{(1)}$ ) with the strongest uplink signal power, and the third null is for FUE ( $\mathbf{h}_{FUE}^{(2)}$ ) with the second strongest uplink signal power. This process is illustrated in Table 4.4.

#### 4.4 Codebook-Based BF (CB-BF)

Since the precoding matrix is stored at each BS to reduce the complexity, we can omit the process of the calculation of weights. Here, we present two algorithms based on the given codebooks [18].

- No PMI Restriction

	<b>FBS</b>	<b>FUE</b>
$t_0$	- Transmits beacon and MIMO pilot on the downlink in each TDD frame.	- Receives beacon and MIMO pilot, and acquires system - Estimate downlink CSI ( $\mathbf{h}_{FUE}^d$ ) based on MIMO pilot.
$t_1$	- Receives reference signal, and obtain downlink CSI ( $\mathbf{h}_{FUE}^d$ ). - Searches the codebook. $\mathbf{q}_r = \arg \max( \mathbf{h}_{FUE}^d \mathbf{q}_r ^2)$	- Transmits reference signal.
$t_2$	- Serves its FUE.	- Receives symbols from serving FBS.

**Table 4.5:** Timing diagram of CB-BF with no PMI restriction

The basic concept of this type of beamforming is the same as TX-BF. Each FBS can obtain the CSI through MIMO and reference pilots. It then searches the codebook for the vector that corresponds to the maximum signal strength of the downlink channel,

$$\mathbf{q}_r = \arg \max_{\mathbf{q}_r \in \mathbf{V}} \|\mathbf{h}_{FUE}^d \mathbf{q}_r\|^2 \quad (4.1)$$

where  $\mathbf{q}_r$  is the selected codeword at the FBS,  $\mathbf{V}$  is the given codebook, and  $\mathbf{h}_{FUE}^d$  is the channel between the FBS and its FUE. Table 4.5 illustrates the process of CB-BF without PMI restriction.

- PMI Restriction

This scheme, initially, was proposed to improve the downlink performance of the cell-edge-user in a multi-cell environment [19]. In this approach, the cell-edge user searches the PMI for codewords that should be restricted to avoid interfering with other users; specifically, the strongest is restricted. This information is then reported to the BS. In this case, there is only one PMI restricted. Obviously, more PMIs can be restricted based on the communication environment.

In a femtocellular environment, the MUE is more vulnerable than the FUE. Therefore, the PMI restriction at the FBS can be utilized to increase MUE performance. The PMI restriction in a femtocellular system is as follows: firstly, the MUE searches the PMI(s) that should be restricted based on the strongest downlink between the FBS and MUE. This PMI information is reported to the MBS, and the MBS shares this information with the FBSs. The restricted PMIs are not used at the FBSs so that the interference at the MUE can be reduced.

#### 4.5 Cooperative Transmission

This algorithm is a new scheme utilizing beamforming with nulling. Often, the FBS is idle, that is, there is no active FUE in the cell. We call such a femtocell on *idle femtocell*. In this case, the idle femtocell should be able to help another FUE that is located in an adjacent femtocell. Since the FBS has low transmit power, this scheme works only when the distances between these FBSs are small. The *cooperative femtocells* are the idle femtocells which help another FUE; here, the serving FBS and the cooperative femtocells transmit the same signal to the desired FUE, simultaneously. Fig. 4.1 illustrates the cooperative transmission concept.

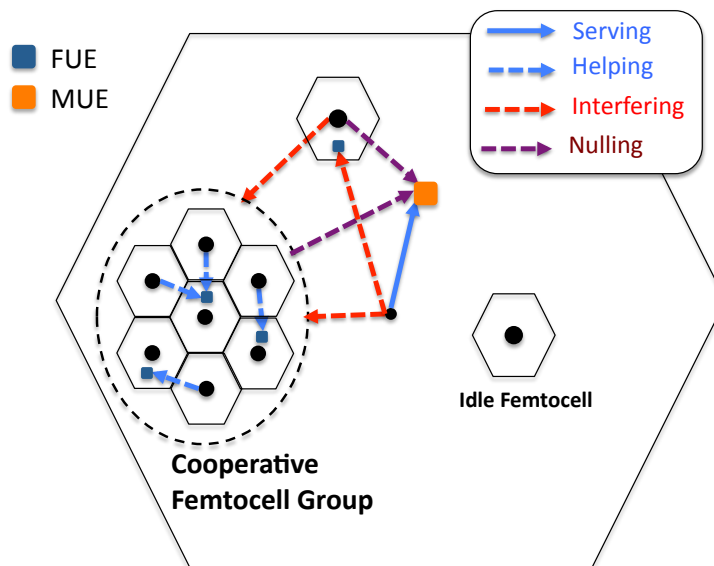


**Figure 4.1:** Cooperative transmission

To implement this algorithm, we assume that the location of each femtocell is known, then the mobile operator can designate a *cooperative femtocell group*. There are two ways to do this: *independent transmission* and *joint transmission*. In independent transmission, the serving FBS and other cooperative femtocells separately perform TX-BF with nulling. For example, two FBSs independently create a beam to the desired FUE and a null to the MUE. As a result, there are two nulls to the MUE which might add and degrade the MUE performance. In this case, the complexity at the BS is relatively low, and phase compensation is not needed. For joint transmission, on the other hand, these two FBSs jointly perform TX-BF with nulling. Therefore, with perfect CSI, there is only one null to the MUE, which is deeper than with independent transmission. However, the complexity at the BS is high due to the required co-phasing of the transmitted signal to compensate for the phase difference between the serving BS and the cooperative BSs [33].

Consider a simple example, in which all of the cooperative femtocells help only one desired user, and in which there is only single macrocell. First, the desired FUE

estimates the phase of each channel from each FBS, then the FUE reports this phase information to the cooperative femtocells. The cooperative femtocells calculate the phase difference between the desired channel and the cooperative channel.

	<b>Cooperative FBS</b>	<b>Active FUE</b>	<b>FUE</b>
$t_0$	- Transmits beacon and MIMO pilot on downlink in each TDD frame.	- Transmits beacon and MIMO pilot on downlink in each TDD frame.	- Receives beacon and MIMO pilot, and acquires system. - Estimates downlink CSI based on MIMO pilot.
$t_1$	- Receives reference signal and identifies strongest FUE and MUE. - Obtains downlink CSI and calculates weight vectors.	- Receives reference signal and identifies desired FUE and MUE. - Obtains downlink CSI and calculates weight vectors.	- Transmits reference signal.
$t_2$	- Serves FUE. (TX-BF with nulling) - Transmits steered reference and carrier pilot.	- Serves FUE. (TX-BF with nulling) - Transmits steered reference and carrier pilot.	- Receives symbols from from FBS(s)

**Table 4.6:** Timing diagram for cooperative transmission

The timing diagram of cooperative transmission, excluding the co-phasing process, is given in Table 4.6.

## Chapter 5

### PERFORMANCE ANALYSIS

In this chapter, we present performance results for the algorithms described in Chapter 4. The common parameters for the simulations are as follows: the carrier frequency =  $2.5\text{ GHz}$ , the thermal noise power =  $-100\text{ dB}$ , and the power of the mobile unit =  $21\text{ dBm}$ . Furthermore, the following table shows the basic parameters for MBS and FBS, respectively. The maximum number of femtocells in a macrocell is 50.

Base Station	No. of Antennas	TX Power	Cell Radius	Antenna Height
MBS	4	$46\text{ dBm}$	$1000\text{ m}$	$10\text{ m}$
FBS	4	$10\text{ dBm}$	$10\text{ m}$	-

**Table 5.1:** Basic parameters for BS

#### 5.1 The Impact of Different Beamforming Techniques

To compare the performance of each beamforming technique, we compute the complementary CDF (CCDF) of the SINR and the spectral efficiency (SE) for different numbers of femtocells in a macrocell. The spectral efficiency (SE) in  $\text{bits/sec/Hz}$  is calculated using the SINR at the receiver and a fixed value for backoff,  $\alpha$ , from the Shannon capacity limit, that is [11][31]:

$$T = \log_2 \left( 1 + \frac{\text{SINR}}{10^{\alpha_{dB}/10}} \right) \quad (5.1)$$

The value of  $\alpha$  can range from 0 to 8 dB, as illustrated in Fig. 5.1. When the transmitter employs adaptive modulation without channel coding,  $\alpha$  can be chosen as 8 dB [11]. Here, assume that  $\alpha$  is 3 dB.

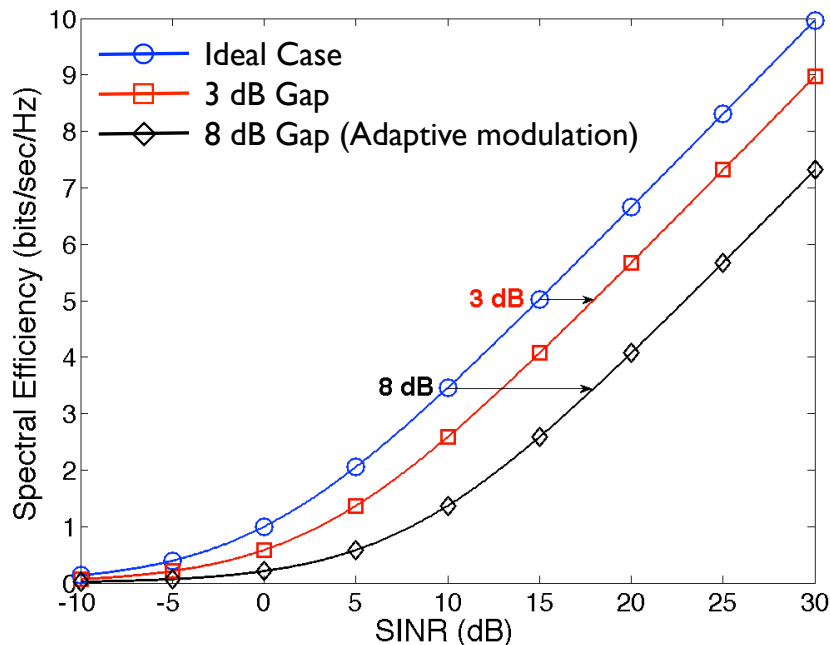


**Figure 5.1:** Comparison of spectral efficiency

### 5.1.1 Macro-User Downlink

Both the CCDF of the downlink SINR and SE for the MUE are shown in Figs. 5.2 and 5.3, assuming 40 FBSs and 50 FBSs, respectively. In the case of TX-BF with nulling, there is one null placed in the direction of the MUE. In every case, TX-BF with nulling is much better than non-beamforming (Non-BF) and TX-BF, and Non-BF and TX-BF have almost the same distribution. Since each FBS places a null to the MUE, the CCI from the FBS can be minimized. In contrast, in Non-BF, the signal is transmitted in all directions. Furthermore, although TX-BF creates a beam in the desired direction, the MUE could be in the direction of the TX-BF beam. Therefore, the MUE performance with TX-BF is not better than

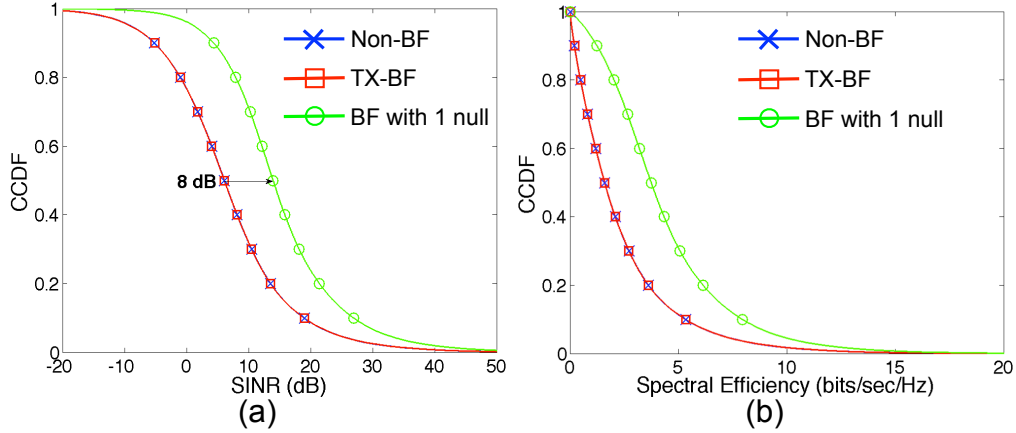


**Figure 5.2:** The CCDF for MUE when 40 FBSs (a) SINR (b) SE

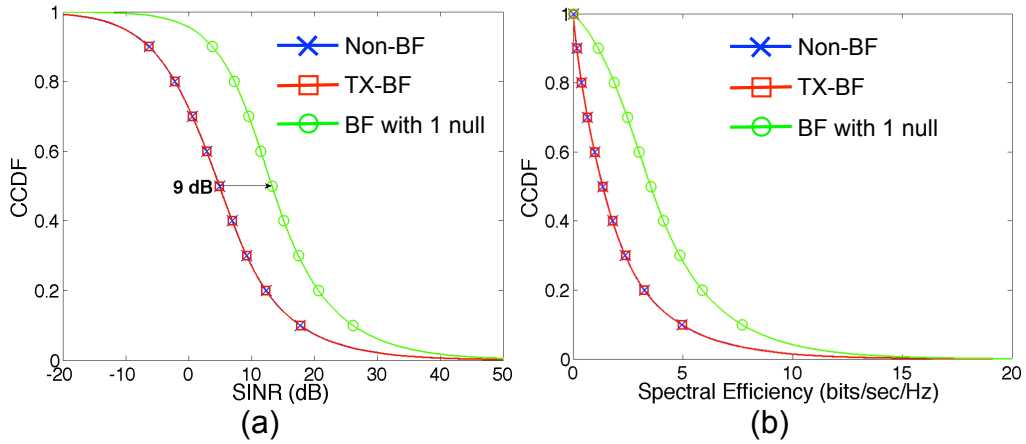


**Figure 5.3:** The CCDF for MUE when 50 FBSs (a) SINR (b) SE

Non-BF. As the number of FBSs increases, the performance of each beamforming technique is generally degraded, but the difference between TX-BF with nulling and both Non-BF and TX-BF is increased. This is because each FBS puts a null in the direction of the MUE, so that the degradation of performance in case of TX-BF with nulling is much lower.

Figs. 5.4 and 5.5 show the SINR and SE of TX-BF with nulling, with the FBS creating different numbers of nulls. As discussed in Chapter 4, more nulls can be created and are based on the uplink signal strength of the mobile user. We fix

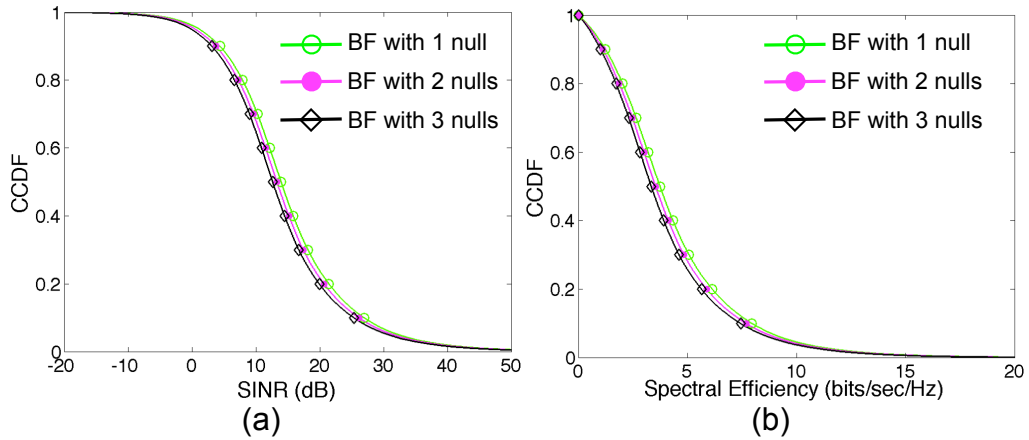


**Figure 5.4:** The CCDF for MUE when 40 FBSs (a) SINR (b) SE

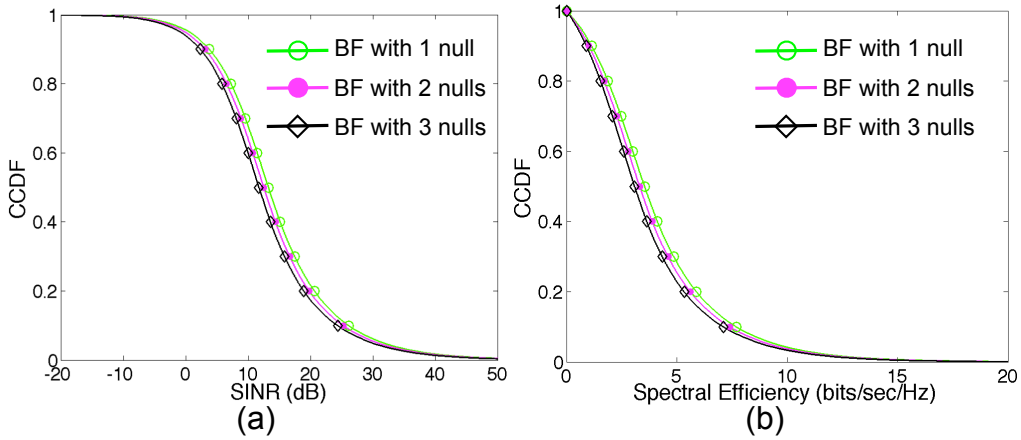


**Figure 5.5:** The CCDF for MUE when 50 FBSs (a) SINR (b) SE

one null for the MUE, and the other nulls are created for the FUEs which have the strongest uplink power. We observe that the SINR of the TX-BF with two or more nulls is slightly lower than the TX-BF with one null; this is because there are not enough transmit antennas (degrees of freedom). Because of this, each FBS cannot create deep nulls in the direction of the MUE and FUE at the same time with only four antennas. Therefore, TX-BF with nulling at only the MUE is a better approach than the other beamforming techniques.

### 5.1.2 Femto-User Downlink

In the case of the FUE, we observe different results from the MUE performance, as shown in Figs. 5.6 and 5.7. Here, TX-BF with nulling and TX-BF are

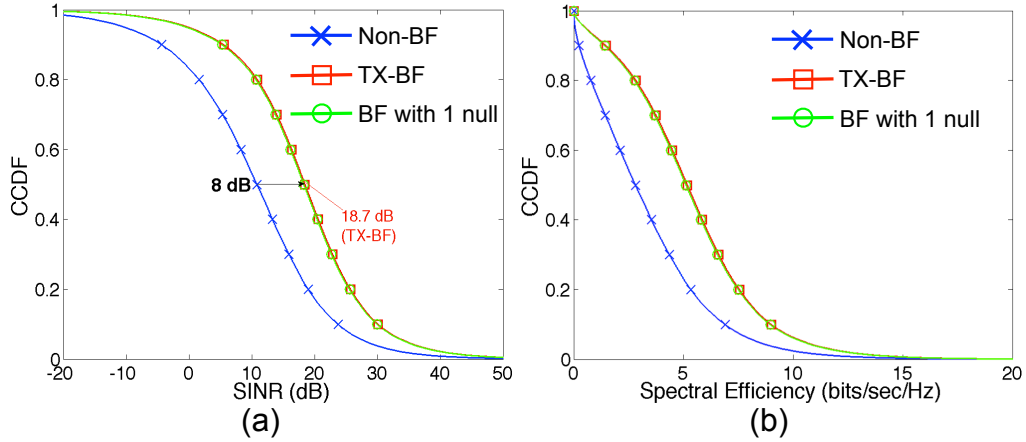


**Figure 5.6:** The CCDF for FUE when 40 FBSs (a) SINR (b) SE

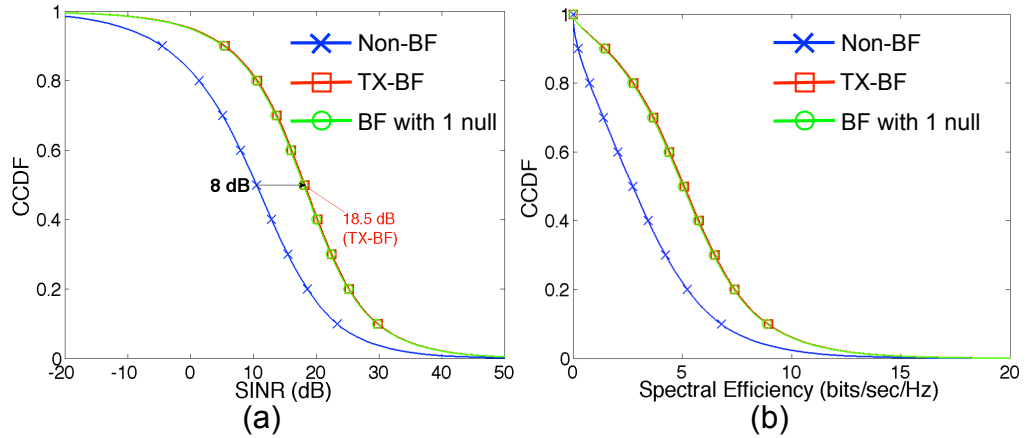


**Figure 5.7:** The CCDF for FUE when 50 FBSs (a) SINR (b) SE

almost identical. Specifically, TX-BF is slightly better than TX-BF with nulling. Since TX-BF with nulling cannot create perfect nulls, interference to the other FUE results. As the number of femtocells increases, the downlink performance at the FUE remains about the same, regardless of the beamforming technique. Likewise,

the difference between TX-BF or TX-BF with nulling and Non-BF does not change. This is because each FBS has low transmit power, so the effect on other FUEs is low, that is, the major interference is from the MBS.

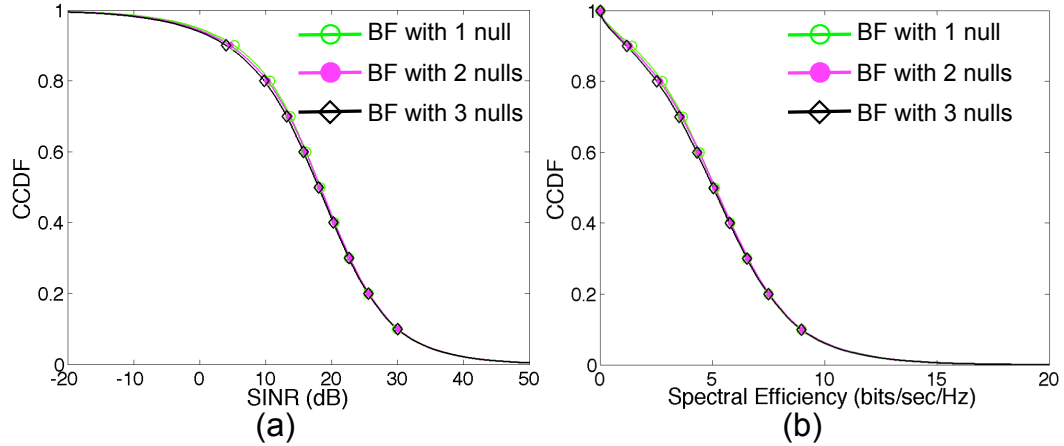


**Figure 5.8:** The CCDF for FUE when 40 FBSs (a) SINR (b) SE

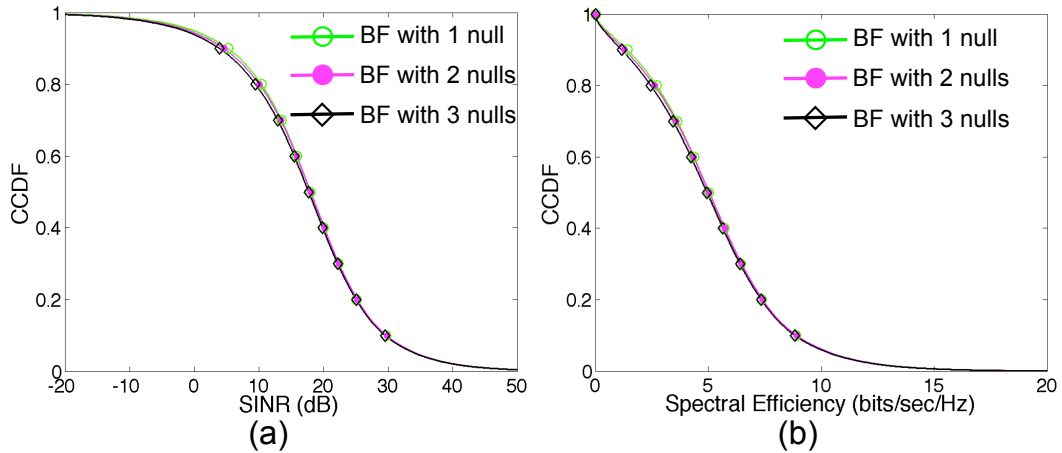


**Figure 5.9:** The CCDF for FUE when 50 FBSs (a) SINR (b) SE

The SINR and SE with different numbers of nulls are shown in Figs. 5.8 and 5.9. These three cases are almost the same. Since there are not enough degrees of freedom, the performance is slightly degraded as the number of nulls increases. However, the differences among these three techniques are small.

Considering both the FUE and MUE downlink, TX-BF with nulling at only the MUE is the best approach to obtain good performance. Creating more nulls, with a fixed number of antennas, provides no benefit for either the FUE or MUE. Instead, the burden of each FBS is increased in terms of the computational complexity and in obtaining the required CSI.

## 5.2 The Impact of Different Numbers of Femtocells

To consider the performance with different numbers of femtocells, we pick the 50% and 10% points of the CCDF of the spectral efficiency.

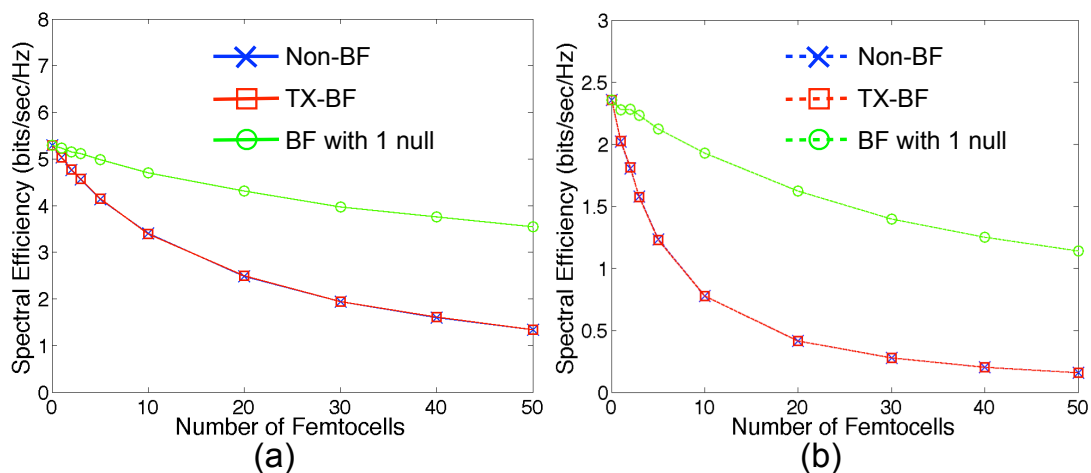


**Figure 5.10:** The SE of MUE with different BF techniques (a) 50% (b) 10%

Figs. 5.10 and 5.11 show the 50% and 10% SE of the MUE for different beamforming techniques and different numbers of nulls, respectively. In the case of TX-BF with nulling, the nulls are created for the MUE and other FUE(s). Both the 50% and 10% SE are generally decreased, and the performance of TX-BF and Non-BF are almost identical, regardless of the number of femtocells. Moreover, as the number of femtocell increases, the MUE performance for Non-BF and TX-BF are greatly degraded. TX-BF with nulling, on the other hand, obtains much better performance than any other techniques due to placing a null at the MUE. In the

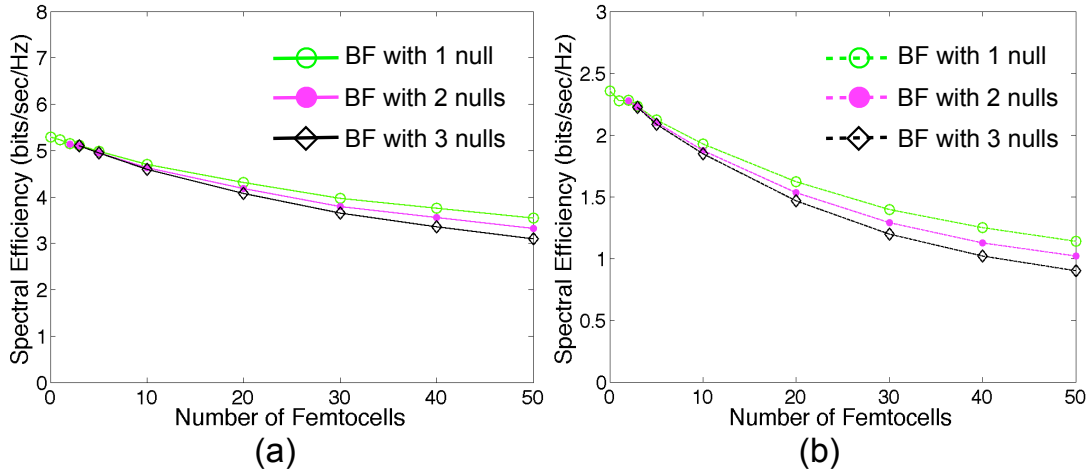


**Figure 5.11:** The SE of MUE with different nulls (a) 50% (b) 10%

case of two or more nulls, TX-BF with nulling at the MUE as well two other FUEs gives the worst performance, especially, when there are a large number of femtocells. This is because there are not enough degrees of freedom.

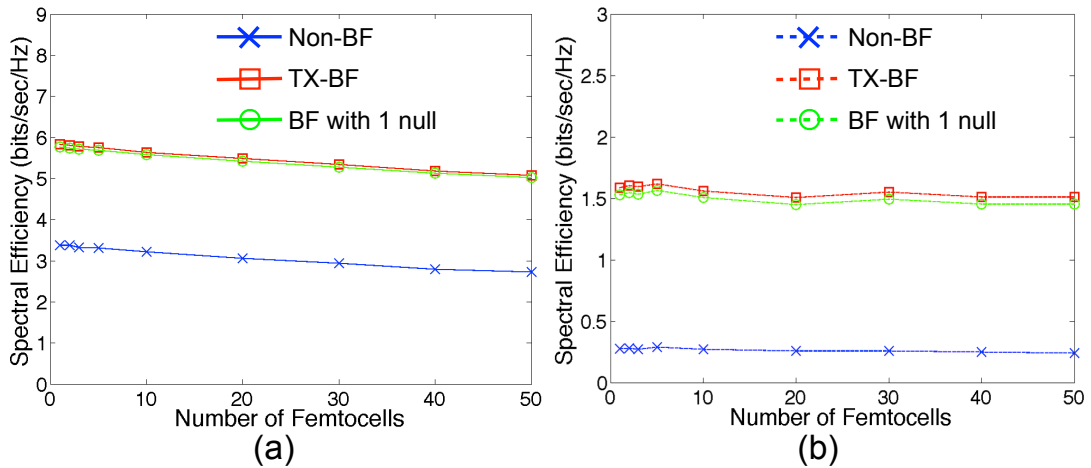


**Figure 5.12:** The SE of FUE with different BF techniques (a) 50% (b) 10%

Figs. 5.12 and 5.13 illustrate the 50% and 10% SE for the FUE. Although the number of femtocells increases, the SE is not degraded much as it was for the MUE performance. In this case, the FUE signal is strong and the CCI from the other FBSs is low. In this sense, we verify the previous result that the major component

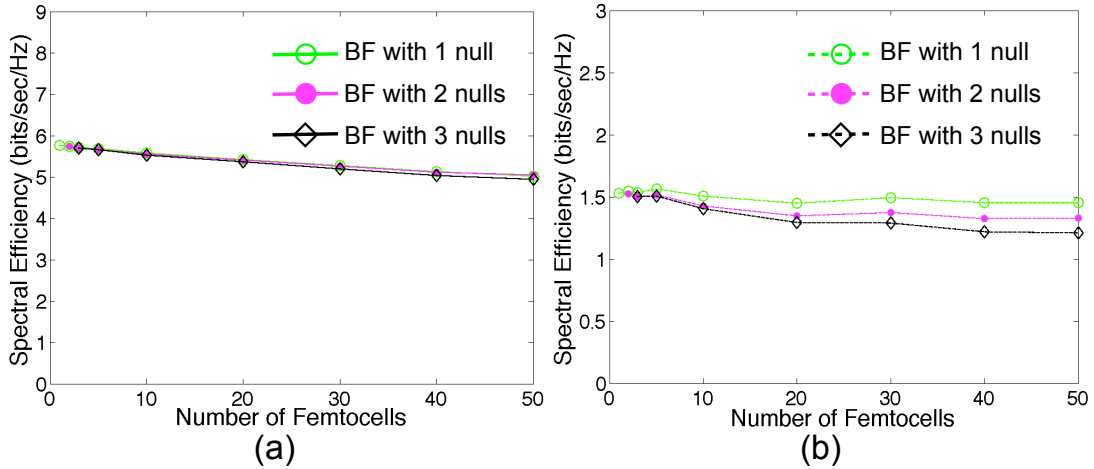


**Figure 5.13:** The SE of FUE with different nulls (a) 50% (b) 10%

of the CCI at the FUE is from the MBS. In addition, with any number of femtocells, the SE of TX-BF and TX-BF with nulling is similar. Specifically, TX-BF is slightly better than TX-BF with nulling, but TX-BF cannot protect the MUE. When each FBS creates two or three nulls for other FUEs, both the 50% and 10% SE of FUE are similar. Specifically, TX-BF with nulling at the MUE and two other FUEs is the worst case again because there are not enough the degrees of freedom. Since each FBS cannot create perfect nulls, they interfere with the FUE. There are no benefits for generating two or three nulls with only four antennas. TX-BF with nulling at the MUE is the best approach for both the FUE and MUE.

### 5.3 The Impact of Different Numbers of Antennas

In this section, we employ different numbers of transmit antennas at the FBS. As mentioned before, the channel capacity increases as the number of the transmit antennas in an i.i.d Rayleigh channel. Here, we employ one, two, and four antennas at the FBS and present the 50% and 10% SE.

Fig. 5.14 illustrates the MUE performance when each FBS employs different

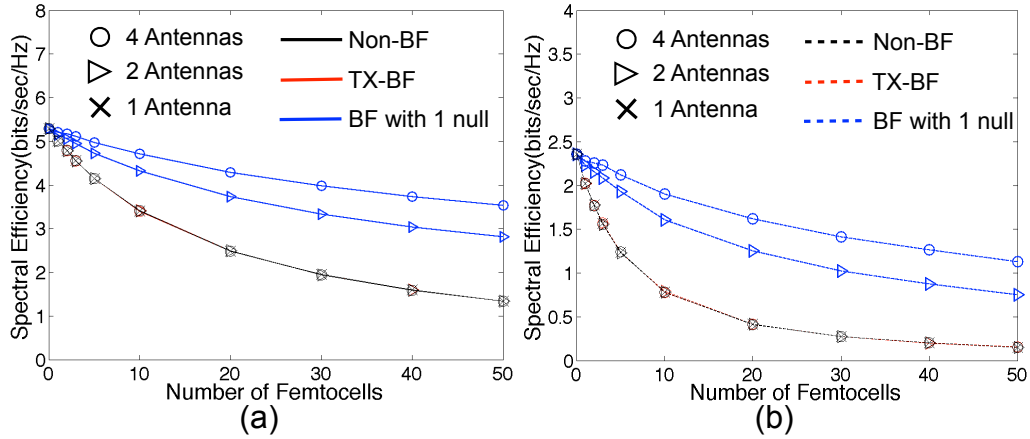


**Figure 5.14:** The SE of MUE with different numbers of antennas (a) 50% (b) 10%

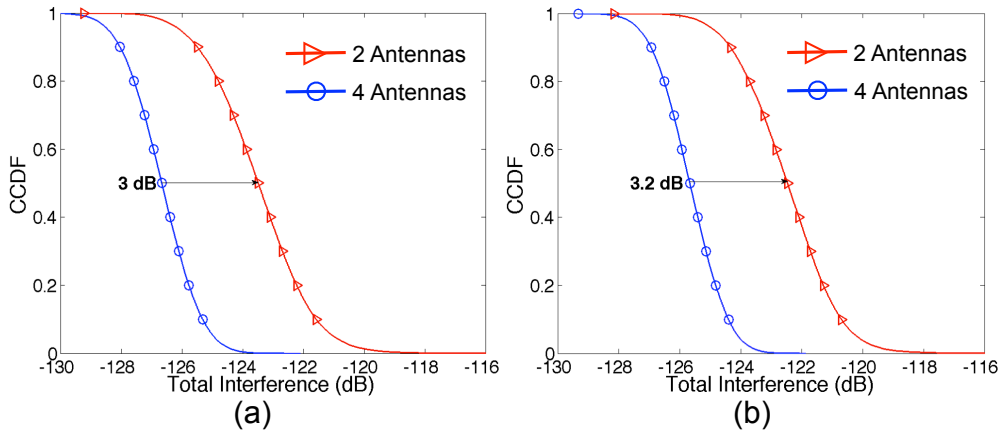


**Figure 5.15:** The CCDF of total interference for 2 and 4 antennas (a) 40 FBSs (b) 50 FBSs

numbers of transmit antennas. Since the MBS performs Non-BF, TX-BF and Non-BF is almost identical, regardless of the number of antennas. In TX-BF with nulling at the MUE, the performance of four antennas is much higher than for two, as expected. Even if a null can be created in the direction of the MUE using two antennas, the CCI from other FBSs employing just two antennas will be higher than in when there are four transmit antennas. To verify this phenomenon, the CCDF of the total interference (in  $dB$ ) is presented in Fig. 5.15. The FUE performance is presented in Fig. 5.16. Generally, the trend of all the curves are the same as the

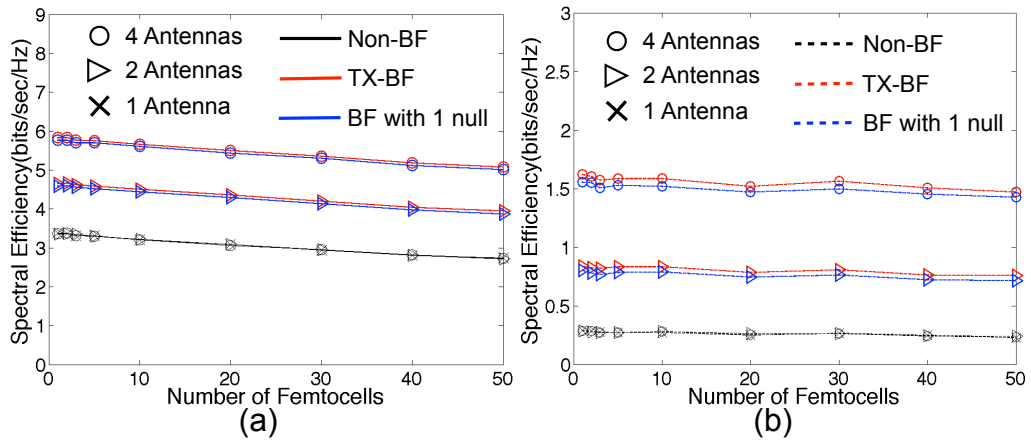


**Figure 5.16:** The SE of FUE with different numbers of antennas (a) 50% (b) 10%

previous FUE results.

## 5.4 Codebook-Based Beamforming (CB-BF)

### 5.4.1 No PMI Restriction

For CB-BF, first we consider the case of no PMI restriction. The MUE performance based on the given codebooks ( $L = 3, L = 6$ ) is shown in Fig. 5.17. In order to compare the performance, TX-BF, TX-BF with nulling, and Non-BF are also presented. All techniques except the BF with nulling at the MUE are essentially

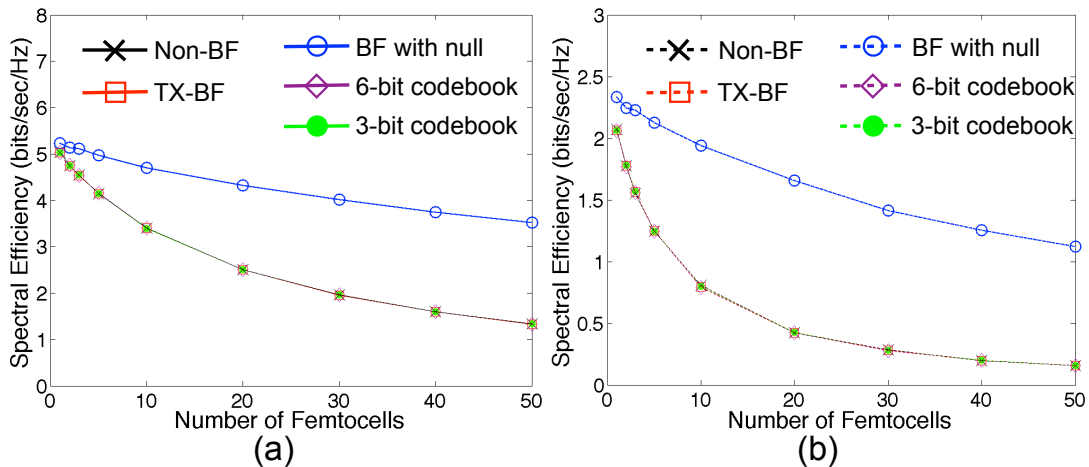


**Figure 5.17:** The MUE performance of CB-BF (a) 50% (b) 10%

identical; this is because there is no interference mitigation for the MUE.

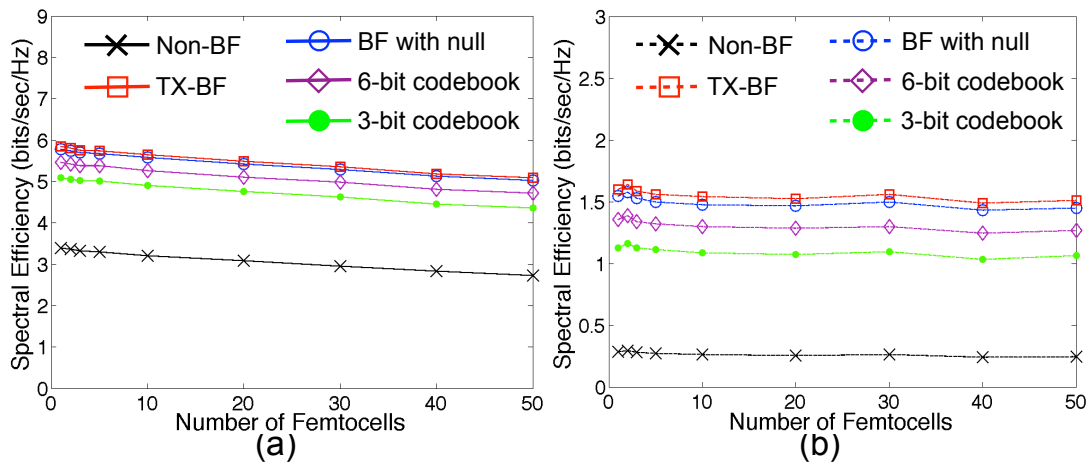


**Figure 5.18:** The FUE performance of CB-BF (a) 50% (b) 10%

On the other hand, the performance of the FUE is very dependent on the beamforming technique. Fig. 5.18 illustrates the FUE performances for 3-bit and 6-bit CB-BF. Since TX-BF and TX-BF with nulling use the optimum weight vectors for the desired user, the performance of both are better than for CB-BF. Furthermore, we can observe that, as expected, beamforming with a 6-bit codebook is better than a 3-bit codebook. This is because, for a 6-bit codebook, the probability is higher that a beam can be formed in the direction to the desired user.

#### 5.4.2 PMI Restriction

In this section, we present the performance of PMI restriction with CB-BF. As mentioned above, the restricted codebooks are generated based on the strength of the interference to the MUE. We compare the performance of PMI restriction with TX-BF with nulling, Non-BF and no PMI restriction. Fig. 5.19 illustrates the MUE performance of PMI restriction with a 3-bit codebook. As observed in previous results, CB-BF with no restriction is almost identical with no beamforming (Non-BF). In PMI restriction, the more codewords that are restricted, the better

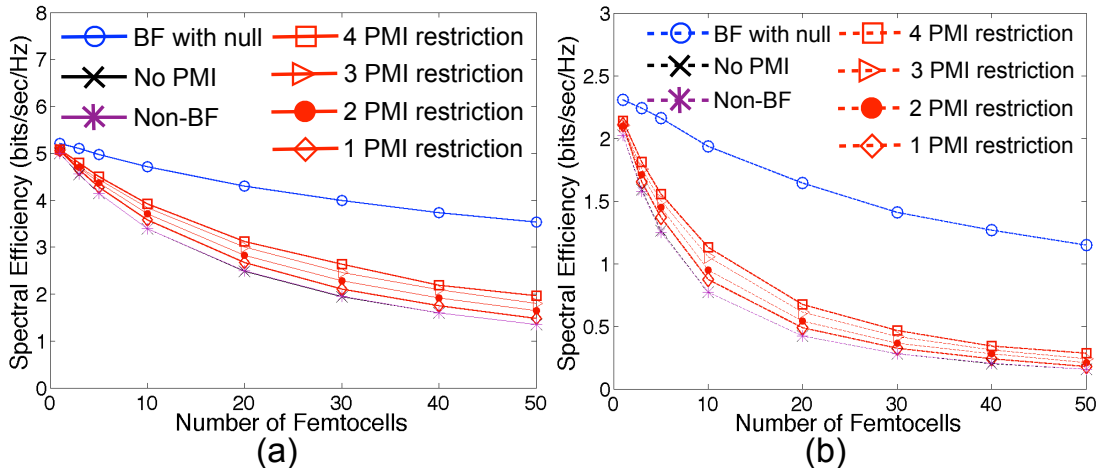


**Figure 5.19:** The MUE performance of 3-bit CB-BF with PMI restriction (a) 50% (b) 10%

the MUE performance. However, we still cannot achieve the TX-BF with nulling performance. Since the size of the codebook is limited, the direction of the beams is always specified. Therefore, the beam direction of the PMI restriction is imperfect. The FUE performance with PMI restriction is shown in Fig. 5.20. In this case,

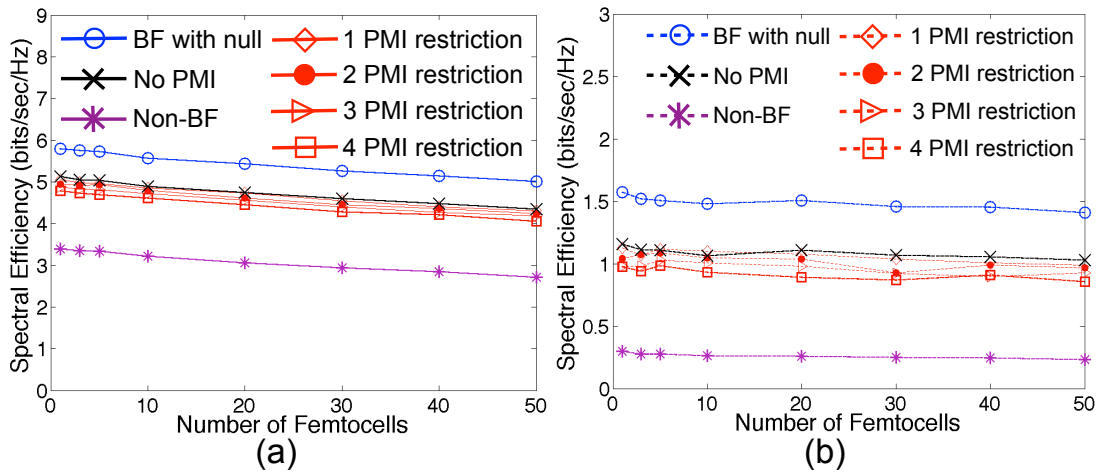


**Figure 5.20:** The FUE performance of 3-bit CB-BF with PMI restriction (a) 50% (b) 10%

the performance with PMI restriction is worse than with no PMI restriction. Likewise, we can observe that as we restrict the size of the codebook, the performance

degrades.

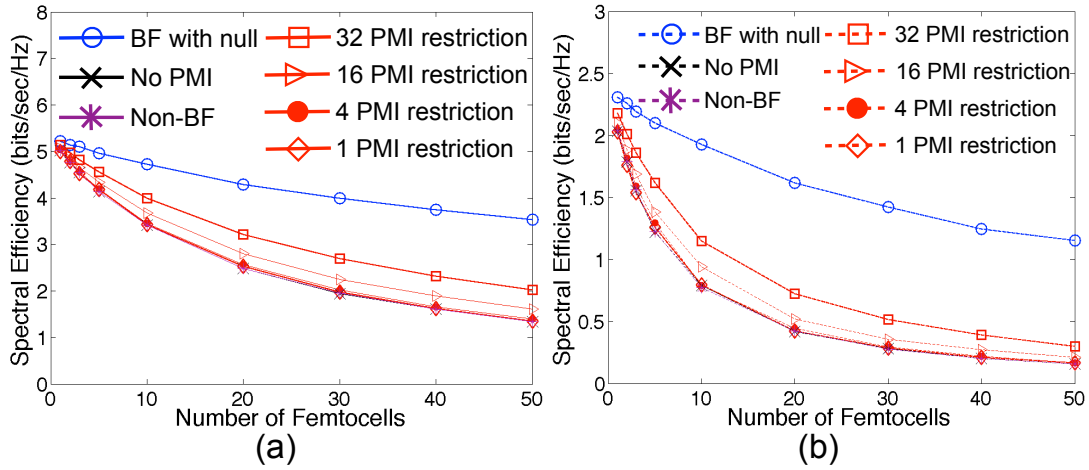


**Figure 5.21:** The MUE performance of 6-bit CB-BF with PMI restriction (a) 50% (b) 10%

Figs. 5.21 and 5.22 show the 50% and 10% SE using a 6-bit CB-BF with PMI restriction. The trend of all results is similar to those with a 3-bit codebook. However, the largest number of PMI restriction is 32, half of all the codewords.

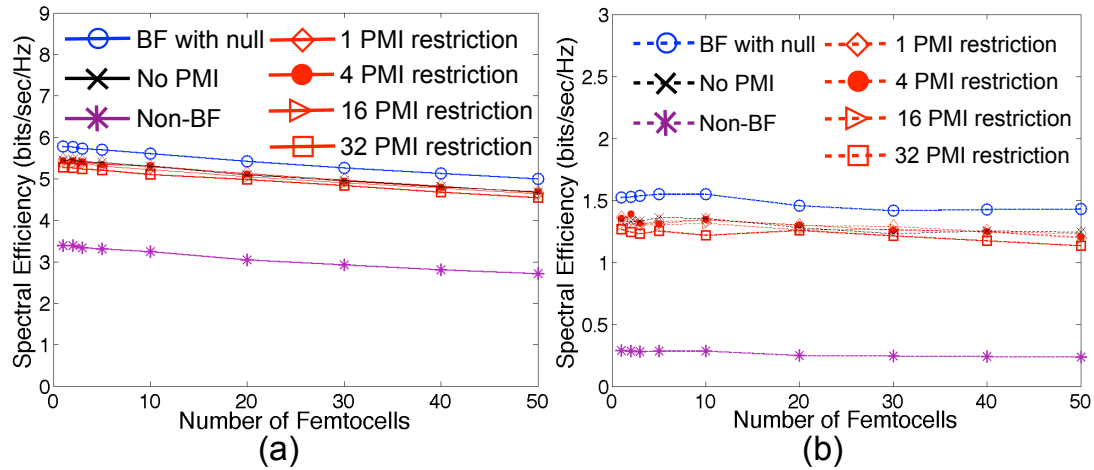


**Figure 5.22:** The FUE performance of 6-bit CB-BF with PMI restriction (a) 50% (b) 10%

## 5.5 The Performance of Cooperative Transmission

The purpose of the cooperative transmission in femtocells is to improve the FUE performance. To implement this, we consider the probability that the FBS is active mode or idle. We introduce the *Poisson distribution* which is the probability of a number of arrivals occurring in a fixed period of time, and is given by

$$P(i) = P(X = i) = e^{-\lambda} \frac{\lambda^i}{i!} \quad (5.2)$$

where  $\lambda$  represents the average number of users in a cell,  $i = 0, 1, 2, \dots$ , and  $E(X) = \lambda$ . In our simulation, the FBS is idle when the value of the Poisson random variable

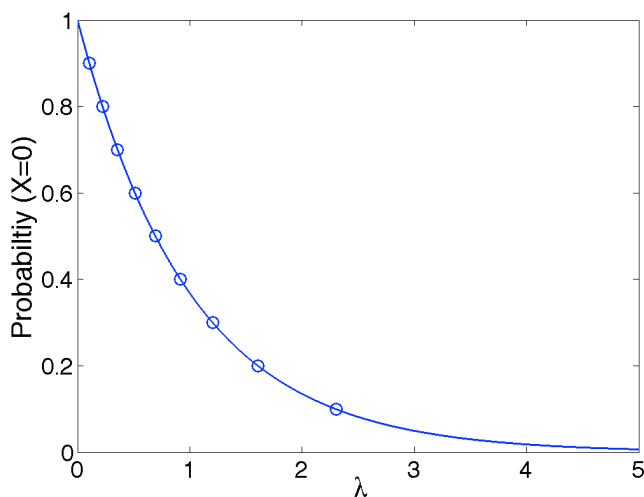


**Figure 5.23:** The Poisson distribution with  $X = 0$  as a function of  $\lambda$

is zero, as shown in Fig. 5.23.

### 5.5.1 The Impact of Cooperative Transmission

As an example, assume that there are up to seven FBSs, and that they are close together. We will call this collection a *cooperative femtocell group*. Assume also that there is only one FUE in the center of the group. Cooperation will only be beneficial if the FBSs are close to each other. The other adjacent FBSs help the desired FUE, and, at the same time, the FBSs put a null in the direction of the

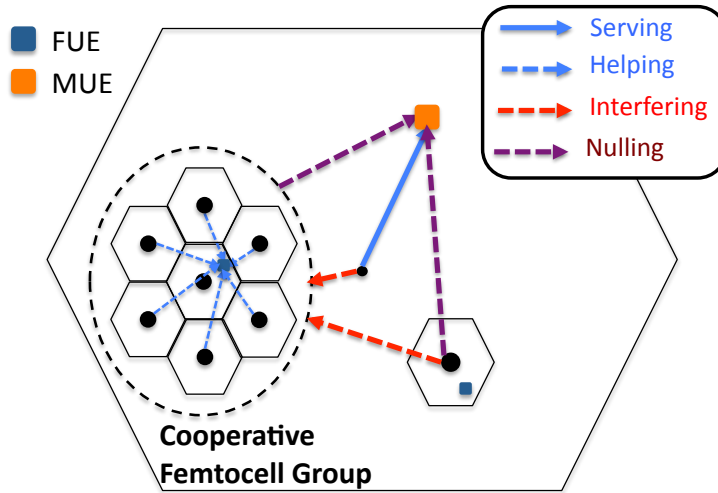


**Figure 5.24:** Femtocell group for cooperative transmission

MUE, as shown in Fig. 5.24. We consider both independent transmission and joint transmission.

Fig. 5.25 illustrates the FUE performance when other FBSs help the desired FUE, assumed to be located in the center of the femtocell group. The other FBSs

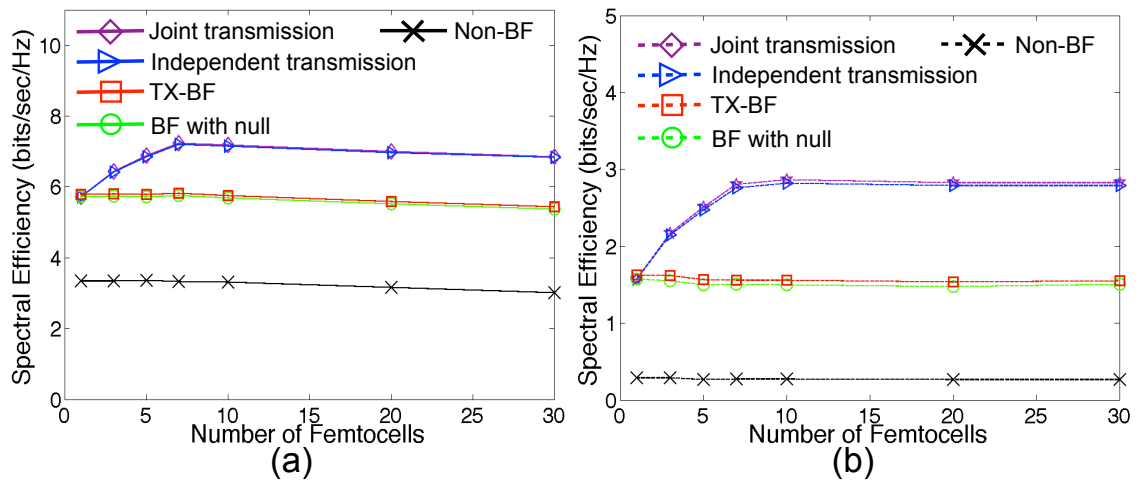


**Figure 5.25:** The FUE performance of cooperative transmission (a) 50% (b) 10%

perform TX-BF with nulling at the MUE. The performance of both TX-BF and TX-BF with nulling are not changed since the main source of the interference is the

MBS. As the number of femtocells increases up to seven FBSs, the performance of cooperative transmission is improved due to the cooperative gain from other femtocells. Independent and joint transmission provide almost identical performance. After seven FBSs, the performance gradually decreases since the last FBSs interferes to the desired user.

The MUE performance is shown in Fig. 5.26. The performance of joint

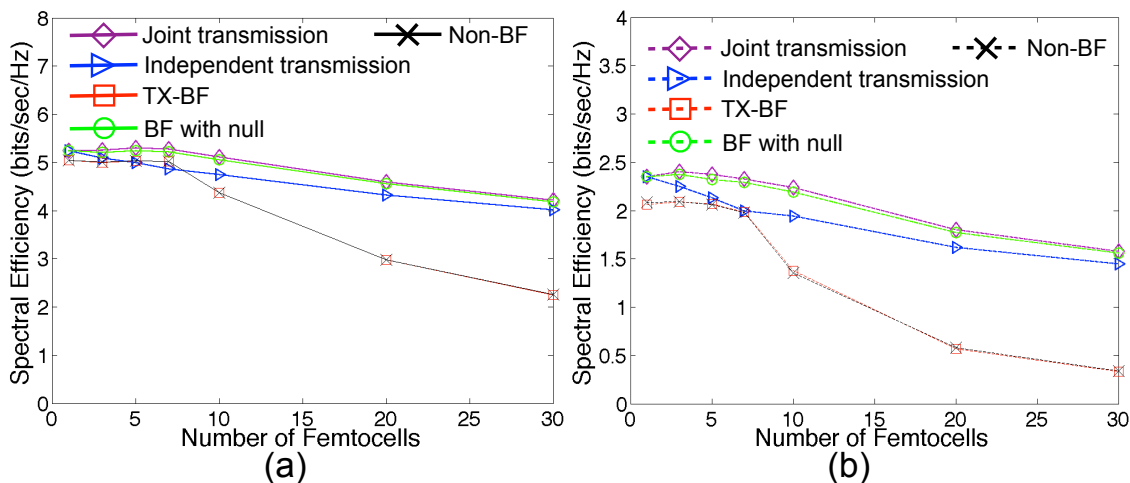


**Figure 5.26:** The MUE performance of cooperative transmission (a) 50% (b) 10%

transmission is very close to TX-BF with nulling, and sometimes even better. This is because joint transmission creates only one null to the MUE and it can be deeper than with TX-BF with nulling and with independent transmission. On the other hand, independent transmission is slightly lower than TX-BF with nulling and even TX-BF or Non-BF within the cooperative femtocell group (around seven FBSs). Each cooperative femtocell creates its own null to the MUE; so this might create more interference to the MUE because each FBS does not have enough degrees of freedom. In TX-BF with nulling, TX-BF, and Non-BF, however, there is only one FBS which is active, and the other six FBSs within the cooperative femtocell group are idle, so the cooperative femtocells no longer cause interference to the MUE. For these reasons, the performance of TX-BF with nulling, TX-BF, and Non-BF is not

changed, and the difference between TX-BF with nulling and TX-BF or Non-BF is so small. Overall, joint transmission is the best approach, however, the computational complexity at the FBS is high compared to the independent transmission, due to the required co-phasing.

### 5.5.2 The Impact of Cell Occupancy

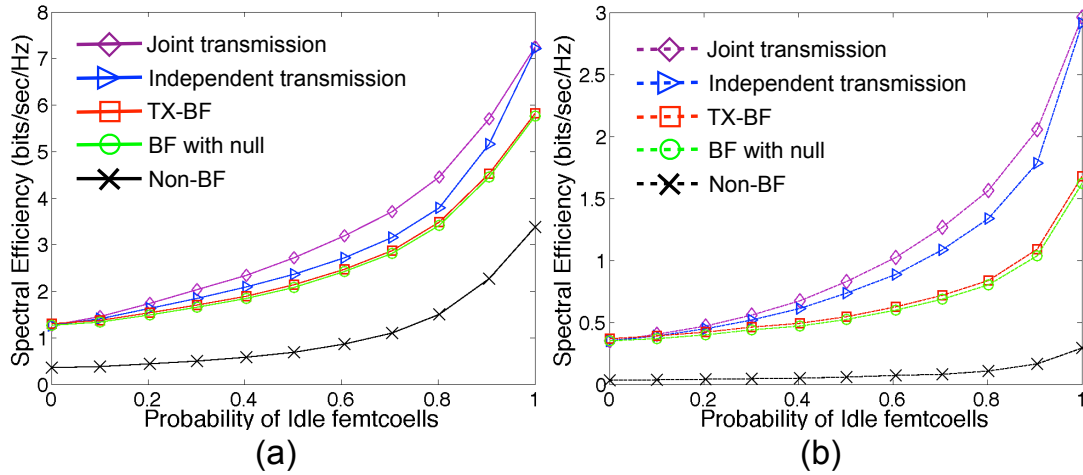


**Figure 5.27:** The FUE performances as a function of the probability of idle FBS (a) 50% (b) 10%

We have shown above that the FUE performance can be dramatically improved as the number of cooperating femtocells increases. In this section, we present the performance variation with the number of femtocells. Figs. 5.27 and 5.28 show the FUE and MUE performance, respectively, when there exists only one cooperative femtocell group (seven FBSs) in a macrocell. Obviously, as the probability of cooperative femtocells increases, the FUE performance will increase. Furthermore, when all of the femtocells have their own FUE to service, the FUE performance will be worse, due to the interference. In the case of MUE performance, as observed before, joint transmission is very close to TX-BF with nulling, regardless of the probability of idle femto cells.

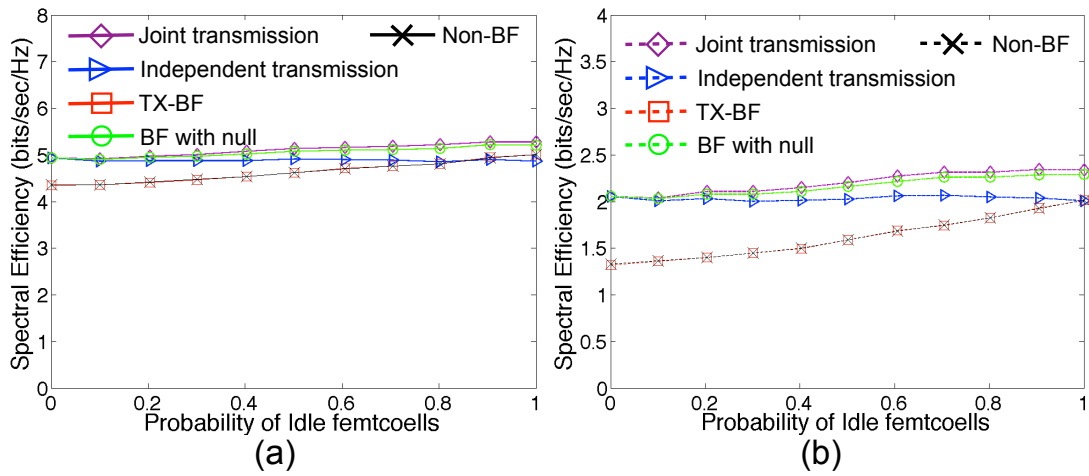


**Figure 5.28:** The MUE performances as a function of the probability of idle FBS (a) 50% (b) 10%

Figs. 5.29 and 5.30 illustrate the FUE and MUE performance, respectively, when 30 femtocells are deployed. In other words, there exist 23 femtocells outside

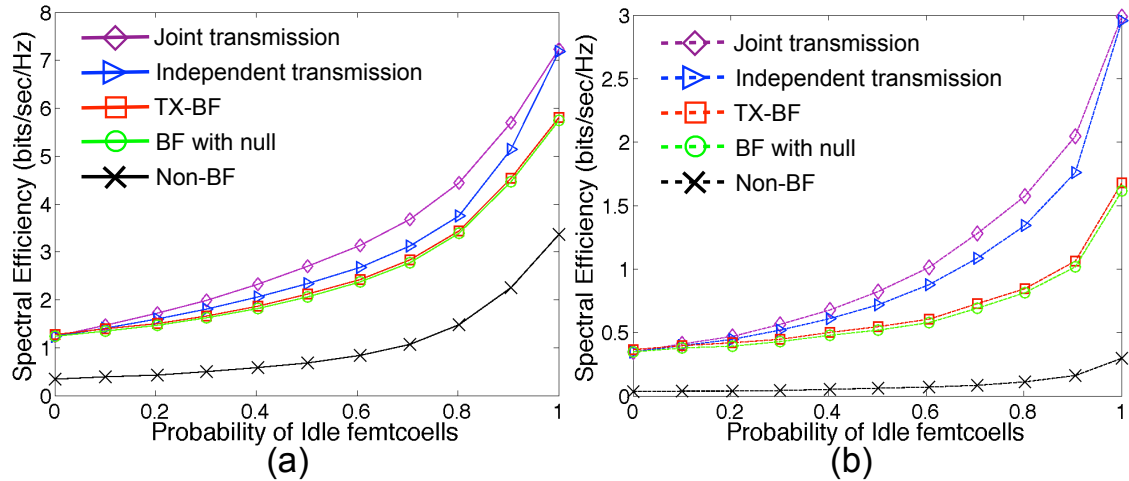


**Figure 5.29:** The FUE performances as a function of the probability of idle FBS (a) 50% (b) 10%

the cooperative group. The trends are identical to those in Figs. 5.27 and 5.28. The

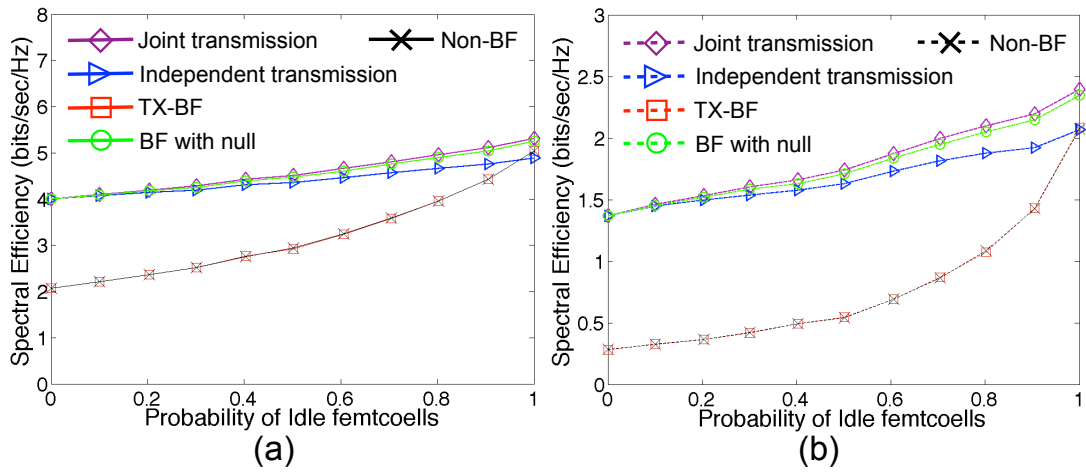


**Figure 5.30:** The MUE performances as a function of the probability of idle FBS  
 (a) 50% (b) 10%

FUE performance is almost identical. The MUE performance, on the other hand, is lower, due to the interference from other FBSs.

## Chapter 6

### CONCLUSIONS AND FUTURE WORKS

In this thesis, we have studied various MIMO beamforming techniques, applied to a femtocellular environment. When each FBS employs multiple antennas, beamforming can greatly improve the FUE performance, regardless of the number of femtocells. Since the FBSs are installed in the existing macrocell, a technique that protects the MUE is required. In this light, TX-BF with nulling at the MUE can obtain the best performance for the FUE while minimizing the interference to the MUE.

CB-BF also can be used for each FBS to reduce the computational complexity. This technique can achieve good performance from the FUE point of view, but the MUE performance is significantly degraded. Although PMI restriction can reduce the interference from each FBS to the MUE, the MUE performance is not significantly improved until half of all the codewords are restricted. Furthermore, as the number of PMI restriction increases to protect the MUE, the FUE performance degrades.

In addition, we have proposed using cooperative transmission among femtocells to improve the FUE and MUE performance at the same time. Specifically, in a high-density femtocellular environment, this technique might be useful. In reality, however, it is hard to form the cooperative group since the use of femtocells is more likely for personal applications.

In this thesis, we have considered a worst-case radio environment. The same carrier frequency is used, so that all of the BSs cause interference. We can also consider some reasonable scheduling algorithm, for example, using a separate frequency for each BS to reduce the CCI. This orthogonalization might be hard to apply in femtocellular environment due to the large number of femtocells. In this sense, an interesting problem is to find the most efficient approach to allocating frequency resources to each FBS.

## BIBLIOGRAPHY

- [1] C. Kennedy, "Wireless in the home and office: the need for both 3G femtocells and Wi-Fi access points," *Femto Forum*, January 2010.
- [2] Femto Forum, <http://www.femtoforum.org/femto/>.
- [3] V. Chandrasekhar, J. Andrews, and A. Gatherer, "Femtocell network: A survey," *IEEE Comm. Mag.*, vol. 46, pp. 59-67, September 2008.
- [4] Femto Forum, "Interference management in UMTS Femtocells," December 2008.
- [5] M. Yavuz, F. Meshkati, S. Nanda, A. Pokhariyal, N. Johnson, B. Raghothaman, and A. Richardson, "Interference management and performance analysis of UMTS/HSPA+ femtocells," *IEEE Comm. Mag.*, vol. 47, no. 9, pp. 102-109, September 2009.
- [6] G. J. Foschini and M. J. Gans, "On limits of wireless communications in a fading environment using multiple antennas," *Wireless Personal Communications*, vol. 6-3, pp. 311-335, 1998.
- [7] E. Telatar, "Capacity of multi-antenna Gaussian channels," *European Trans. on Telecom.*, November 1999.
- [8] A. Goldsmith, N. Jindal, and S. Vishwanath, "Capacity limits of MIMO channels," *IEEE J. on Sel. Areas in Commun.*, vol. 21, no. 5, pp. 684-702, January 2003.
- [9] S. Catreux, P. F. Driessen, and L. J. Greenstein, "Data throughputs using multiple-input multiple-output (MIMO) techniques in a noise-limited cellular environment," *IEEE Trans. on Commun.*, vol. 1, no. 2, pp. 226-235, April 2002.
- [10] S. Catreux, L. J. Greenstein, and V. Erceg, "Some results and insights on the performance gains of MIMO systems," *IEEE J. on Sel. Areas in Commun.*, vol. 21, no. 5, pp. 839-847, June 2003.

- [11] S. Catreux, P. F. Driessen, and L. J. Greenstein, "Simulation results for an interference-limited multiple-input multiple-output cellular system," *IEEE Commun Letters*, vol. 4, no. 11, November 2000.
- [12] S. Catreux, P. F. Driessen, and L. J. Greenstein, "Attainable throughput of an interference-limited multiple-input multiple-output (MIMO) cellular system," *IEEE Trans. on Commun.*, vol. 49, no. 8, pp. 1307-1311, August 2001.
- [13] A. Maaref and S. Aissa, "Closed-form expressions for the outage and ergodic Shannon capacity of MIMO MRC systems," *IEEE Trans. on Commun.*, Vol. 53, No. 7, pp. 1092-1095, July 2005.
- [14] W. C. Wong and S. Talwar, "Interference mitigation using downlink transmit beamforming with nulling techniques", *IEEE C802.16m-08/653r2*, July 2008.
- [15] B. M. Hochwald and T. L. Marzetta, "Unitary space-time modulation for multiple-antenna communications in Rayleigh flat fading," *IEEE Trans. on Inform. Theory*, vol. 46, no. 2, pp. 543-564, March 2000.
- [16] B. M. Hochwald, T. L. Marzetta, and T. J. Richardson, W. Sweldens, "Systematic design of unitary space-time constellations," *IEEE Trans. on Inform. Theory*, vol 46, no. 6, pp. 1962-1973, September 2000.
- [17] J. C. Roh and B. D. Rao, "Design and analysis of MIMO spatial multiplexing systems with quantized feedback," *IEEE Trans. on Sig. Proc.*, vol. 54, no. 8, pp. 2874-2886, August 2006.
- [18] Q. Li, X. E. Lin, and J. Zhang, "MIMO precoding in 802.16e WiMAX," *J. of Commun. and Net.*, vol. 9, no. 2, pp. 141-149, June 2007.
- [19] D. Lim, S. Kim, J. Kim and B. C. Ihm, "PMI restriction for the downlink closed-loop MIMO," *IEEE C802.16m-08/430r1*, July 2008.
- [20] D. N. Knisely, T. Yoshizawa, and F. Favichia, "Standardization of femtocells in 3GPP," *IEEE Comm. Mag.*, vol. 47, no. 9, pp. 68-75, September 2009.
- [21] D. N. Knisely, and F. Favichia, "Standardization of femtocells in 3GPP2," *IEEE Comm. Mag.*, vol. 47, no. 9, pp. 76-82, September 2009.
- [22] R. Y. Kim, J. S. Kwak, and K. Etemad, "WiMAX femtocell: Requirements, challenges, and solutions," *IEEE Comm. Mag.*, vol. 47, no. 9, pp. 84-91, September 2009.
- [23] S. P. Yeh, S. Talwar, S. C. Lee, and H. C. Kim, "WiMAX femtocells: A perspective on network architecture, capacity, and coverage," *IEEE Comm. Mag.*, vol. 46, no. 10, pp. 58-65, October 2008.

- [24] C.E. Shannon, "A mathematical theory of communication," *Bell Sys. Tech. J.*, vol. 27, pp. 379-423, 623-656, July, October 1948.
- [25] A. Goldsmith, *Wireless Communication*. Cambridge University, 2005.
- [26] REPORT ITU-R M.1225, "Guidelines for evaluation of radio transmission technologies for IMT-2000."
- [27] IST-4-0277560 WINNER II deliverable d1.1.2 v1.1, "WINNER II channel models."
- [28] REPORT ITU-r m.2135, "Guidelines for evaluation of radio interface technologies for IMT-advanced."
- [29] L. T. W. Ho and H. Claussen, "Effects of user-deployed, co-channel femtocells on the call drop probability in a residential scenario," *The 18th IEEE Inter. Symp. on PIMRC 2006*, pp. 1-5, September 2006.
- [30] K. Lee, J. Ko, and Y.-H. Lee, "Downlink beamforming for other cell interference mitigation in correlated MISO channel," *European Wireless Conference*, April. 2007.
- [31] H. Claussen and A.L. Swindon, "Performance of macro- and co-channel femtocells in a hierarchical cell structure," *PIMRC 2007*, pp. 1-5, September 2007.
- [32] J. W. Ketchum, M. S. Wallace, J. R. Walton, and S. J. Howard, "Pilots for MIMO communication systems," *US Patent*, September.16.2004.
- [33] K. W. Lee, and Y. H. Lee, "Cooperative transmission with partial channel information in multi-user MISO wireless systems," *IEEE VTC 2008*, September 2008.